Photo-oxidation and weathering of LDPE studied by surface and bulk analysis

vorgelegt von

MSc. Maalolan Ramanujam

aus Tiruchirapalli, Indien

von der Fakultät III - Prozesswissenschaften

der Technischen Universität Berlin

zur Erlangung des akademischen Grades

Doktor der Naturwissenschaften

Dr. rer. nat.

genehmigte Dissertation

Promotionsausschuss:

Vorsitzender:	**Prof. Dr. Bernhard Senge**
Gutachter:	**Prof. Dr. rer. nat. Jörg F. Friedrich**
Gutachter:	**Prof. Dr. -Ing. Manfred H. Wagner**

Tag der wissenschaftlichen Aussprache: 14-12-2012

Berlin 2013

D83

Declaration

I hereby declare that my Dissertation work titled ***Photo-oxidation and weathering of LDPE studied by surface and bulk analysis*** is completely an independent work and I have not used any sources or references that are not cited.

23.09.2012 Maalolan Ramanujam.

Berlin

To my parents, Mr. S. Ramanujam & R. Vaidehi,

Grandmother, S. Pankajam,

Wife, Pooja.

Acknowledgement

First and foremost, I thank the German Government, University of Stuttgart, TU Berlin and BAM for giving me a wonderful opportunity to continue my studies and realize my dreams.

I am deeply grateful to Prof. Dr. rer. nat. Jörg F. Friedrich for his valuable suggestions and advises for completing the thesis work and without his guidance this work would not have been possible.

I sincerely thank Prof. Dr.-Ing. Manfred Wagner for his guidance and advises in PhD work plan which helped me to complete the work in time. I'm very fortunate to have him as my supervisor. He supported me in all possible ways whenever I faced hurdles in getting along with the work.

I would like to thank Dr. rer. nat. Renate Mix for her support and motivation.

I thank Prof. Dr. Andreas Schönhals for his guidance for the DRS measurements which is the building block of the thesis. Without his mentoring, my first publication would not have been possible.

Special thanks to Dr. rer. nat. Volker Wachtendorf for gracefully allowing me to use the artificial weathering chamber. He patiently entertained long discussions in spite of his busy schedule. I thank Mrs. Gundula Hidde, Mr. Frank Milczewski, Mr. Dietmar Neubert, Mrs. Ziemann, and Dr. Gerhard Kalinka for their support in using different analytical methods.

I thank all the members of the Department 6.10 for supporting me all these 3 years. There is always a special place in my heart for all my friends and well-wishers like Ramasubramanian, Lakshmi Narasimhan, Srinivasan, Purv, Kishore, Huajie, Mishra and Kumar for their constant support and motivation right throughout the PhD.

I thank my parents, brothers, my sweet nieces Sumithrai, Mridula and grandmother at this point. They have always been my pillar of support.

There is a special person in my life and she is none other than my wife Pooja Santhanam. Since I'm a difficult person to live with, her presence has always been a symbol of support. God knows whether she understood or not my scientific problems, but she had enough patience to listen and cheer me all the time. Thank you dear!

The knowledge and experience gained during these 7 years of stay in Germany cannot be expressed in 1 or 2 pages, but I would conclude that it definitely gave me the confidence to survive in this competitive world.

Table of contents

List of abbreviations

Ar	Argon
ASTM	American Society for Testing and Materials
Br	Bromine
°C	Degree centigrade
DSC	Differential scanning calorimetry
DRS	Dielectric relaxation spectroscopy
DPPH	2,2,-diphenyl-1-picrylhydrazyl
ΔH	Enthalpy of melting
ESR	Electron spin resonance
F	Frequency
FTIR-ATR	Fourier transform Infra-red-Attenuated total reflectance
G	Gauss
HN	Havriliak-Negami
HDPE	High density polyethylene
HALS	Hindered amine light stabilizers
Hz	Hertz
h	hour
K	Kelvin
LDPE	Low density polyethylene
min	minute
NO	Nitric oxide
O	Oxygen
PE	Polyethylene
RH	Relative humidity
RF	Radio frequency
RH	Organic material
sccm	Standard cubic centimeter
s	second
TEMPO	2,2,6,6,-tetramethylpiperidine-N-oxide
UV-vis	Ultraviolet-visible

UV	Ultraviolet
VFT	Vogel-Fulcher-Tammann
VUV	Vacuum ultra violet
W	Watt
XPS	X-ray photoelectron spectroscopy
$\pi \rightarrow \pi^*$ transitions	Transition of an electron from bonding π orbital to anti-bonding π^* orbital
$\sigma \rightarrow \sigma^*$ transitions	Transition of an electron from bonding σ orbital to anti-bonding σ^* orbital

Abstract

Low density polyethylene (LDPE) is one of the cost-effective and an often used polymer in packaging industries and in our day-to-day life. Their instability towards UV radiation and mechanism of photo-degradation is still under debate. The aim of this work is to understand the effect of photo-oxidation on LDPE induced by weathering. In this dynamic world, "faster and reliability" are the two important factors that decide the success of any testing method.

Artificial weathering has been widely used in the place of outdoor weathering, which reduced the time significantly from years to days. However, with proper testing method the days could also be reduced to hours. In this regard, oxygen plasma weathering can be a reliable method in simulating the effects of artificial weathering. In this dissertation, the photo-oxidation at various layers of the LDPE induced by artificial weathering and oxygen plasma weathering have been explored and analyzed by various surface and bulk techniques.

The artificial weathering tests were carried out in a weathering chamber with the temperature set at 60°C under two different humid conditions: at <15% and >90% RH. It was found that the LDPE foils of 40 µm thickness could not be weathered after 32 days under <15% RH and whereas at >90% RH the foils could not withstand beyond 12 days. In both the cases, foils seem to lose their structural integrity due to embrittlement. This work discusses in detail how the foil reaches this stage of embrittlement for two different humid conditions based on XPS, FTIR and dielectric data assisted with the DSC. It was also found that it is possible to track the processes that are responsible for degradation and discusses how dielectric spectroscopy could be used to understand the mechanical disintegration due to artificial weathering.

In the past, few studies have been conducted and it was found that it is possible to correlate the effects of outdoor weathering with oxygen plasma treatments. In this study, oxygen plasma was used to irradiate LDPE for longer time periods to see if there is any similarity with the effects of artificially weathered LDPE. It was found that only by XPS the comparisons of surface oxidations are possible. On the contrary, there is no significant change in the ATR-FTIR spectra within its sampling depth of 2.5 µm. The micro-tensile

measurements also show that materials are ductile in nature and with 4h of plasma treatment the ductility decreases. No correlation of results with artificial weathering achieved using FTIR and micro tensile studies.

Since the plasma weathering is largely surface effect, a method was tried to modify the polymer surface by bromine gas after argon plasma treatment and to check for changes in the surface photo-oxidation. It was found by XPS that, the bromination does not reach the same sampling depths as oxygen and it reacts with many radicals and hinders /slows down the auto-oxidation process at ambient pressure. Using the same XPS data, double bonds concentrations have been calculated which is in agreement with the literature.

Finally, the classic solution of using stabilizers was also studied. UV in-situ weathering with simultaneous ESR measurement was used. It was found that for unstabilized LDPE the radical intensity decreases with increase in UV irradiation time. In contrast, for Hostavin N30 stabilized LDPE the radical intensity increases with time showing good protection against UV radiation.

Zusammenfassung

Nieder dichte Polyethylene (LDPE) ist ein kostengünstiges und ein deshalb oft in der Verpackungsindustrie genutztes Polymer. Seine Instabilität gegenüber UV-Strahlung ist nachteilig. Diese Arbeit ist ein Versuch, die Wirkung der Photo-Oxidation von LDPE zu verstehen und den Mechanismus der durch Bewitterung induzierten Veränderungen zu identifizieren. Die künstliche Bewitterung und die damit verbundenen photo-oxidativen Veränderungen im Polymer werden seit Jahrzehnten erforscht, jedoch sind die photo-physikalischen und photo-chemischen Prozesse an der Oberfläche und in unmittelbarer Nähe zur Oberfläche weiterhin Gegenstand von Untersuchungen und Diskussionen. In dieser Arbeit wurde die Photo-Oxidation in verschiedenen Schichten des LDPE durch künstliche Bewitterung (UV-C, Temperatur, Luftfeuchte), durch Sauerstoffplasmaexposition einschl. der dabei auftretenden Vakuum-UV-Strahlung sowie durch UV-Bewitterung und In-situ-Verfolgung mittels Elektronen-Spinresonanz (ESR) charakterisiert, wobei weitere Oberflächen- und Volumen-Analysenmethoden eingesetzt wurden. Die künstlichen Bewitterung wurde in einer Bewitterungskammer mit kontinuierlich emittierenden Fluoreszenzlampen im UV-A-Bereich, bei einer Temperatur von 60° C und bei zwei verschiedenen Feuchtebedingungen durchgeführt und zwar bei <15% und bei > 90% relative Luftfeuchtigkeit (RH). Um zu verstehen, wie die Photo-Oxidation der Oberfläche und die Volumeneigenschaften voneinander abhängen, wurden folgende Analysentechniken eingesetzt: Photoelektronenspektroskopie (XPS), Fourier-Transform Infrarot Spektroskopie (FTIR) mittels abgeschwächter Totalreflektion (ATR) als Methoden mit geringen Informationstiefen an der Oberfläche und Volumenmethoden, die das gesamte Probenvolumen erfassen, wie Dielektrische Relaxationsspektroskopie (DRS) und Differential Scanning Calorimetry (DSC).

Die XPS-, aber auch die ATR-FTIR Untersuchungen der Photo-Oxidation an der Polymeroberfläche im Klimaschrank zeigten eine erhöhte Konzentration an Sauerstoff-

enthaltenden funktionellen Gruppen. In der ersten Bewitterungsphase gibt es keine Änderung im Volumen des Polymers. Die typische Volumenmethode DRS bestätigt jedoch, daß durch die Bildung von Radikalen, Anlagerung von Sauerstoff und Bildung von Peroxyradikalen und weiteren Folgeprodukten an der Polymeroberfläche genügend dielektrisch aktive Relaxationsprozesse mit veränderter Intensität zu beobachten sind, die auch bereits im nichtbewitterten LDPE zu erkennen sind. Bei etwas längerer Bewitterung sind deutlich erhöhte dielektrische Verluste durch molekulare Schwingungen in den amorphen und kristallinen Bereichen des Polymers zu erkennen. Aktivierungsenergien und dielektrische Verluste wurden für jeden einzelnen Prozess ermittelt. Es wurde festgestellt, dass die 40 µm dicken LDPE-Folien nicht länger als 32 Tage bei <15% RH und nicht mehr als 12 Tage bei >90% RH bewittert werden konnten. Über die genannten Bewitterungszeiträume hinaus versprödeten die Folien derart, daß sie zerfielen. Neben der DRS wurden die Proben bis zur Versprödung auch mittels DSC charakterisiert. Die entsprechenden, für den Abbau bis hin zur Versprödung verantwortlichen Prozesse bei der künstlichen Bewitterung werden diskutiert.

Es gab frühere Ansätze, die natürliche bzw. künstliche Bewitterung von Polymeren durch eine Exposition der Polymerproben in einem Sauerstoff-Niederdruckplasma extrem zeitgerafft zu simulieren, was vor allem bei LDPE Erfolg hatte. Als Hauptwirkungsfaktor bei der ultraschnellen Alterung wurde die extrem kurzwellige Vakuum-UV-Strahlung identifiziert. Hier wurde das Sauerstoffplasma verwendet, um LDPE über längere Zeiträume dem Bombardement mit energiereichen Plasmaspezies und der Vakuum-UV-Strahlung auszusetzen, um dann zu sehen, ob es eine Ähnlichkeit mit der natürlichen bzw. der Klimakammer-Bewitterung gibt. ATR-FTIR und XPS wurden verwendet, um die Oxidation der Oberfläche zu studieren. Die Zugfestigkeit der plasmaexponierten Proben wurde gemessen, um die Volumen-Eigenschaftsänderungen zu prüfen. Es wurde gefunden, dass nur durch die XPS-Oberflächenanalytik die Oberflächenoxidation eindeutig nachweisbar ist. Wird die ATR-FTIR-Technik eingesetzt, die eine Informationstiefe von 2,5 µm besitzt, im Gegensatz zu der der XPS mit 0,006 µm, sind kaum mehr Indizien für eine Oberflächenoxidation zu erkennen. Bei kurzen Behandlungszeiten im Sauerstoffplasma

wurden keine Veränderungen beobachtet. Die Zugfestigkeits-/Dehnungs-Messungen zeigten auch, dass nach 4 h Plasmabehandlung die Duktilität abnimmt. Da die „Plasma-Bewitterung“ weitgehend ein Oberflächeneffekt ist und dabei die plasmaerzeugten Kohlenstoffradikale eine große Rolle spielen, wurde die Bromierung der Radikale als Derivatisierungsmethode eingesetzt, um deren Konzentration durch die Menge des gebundenen Broms bestimmen zu können. Die chemische Bromierung durch Quenchen der C-Radikale an der Polymeroberfläche nach Argon-Plasma-Behandlung und Bromdampfzugabe erreicht nicht die gleichen Probentiefen wie das Sauerstoffplasma, wie winkelaufgelöste XPS-Messungen ergaben. Die Reaktion zwischen Brom und C-Radikalen unterbindet auch das Fortschreiten von Autoxidationsprozessen beim Lagern der plasmabehandelten Proben an Luft. Neben der Radikalentstehung wurde auch die Bildung von erheblichen Konzentrationen an C=C-Doppelbindungen bei der Behandlung im Argonplasma beobachtet, wie die XPS- und UV-spektroskopischen Messungen belegten.

Die strukturellen und kompositorischen Veränderungen nach künstlicher Bewitterung wurden mit denen nach Sauerstoff- oder Argon-Plasmabehandlung, aber auch nach UV-Bestrahlung verglichen. Die UV-Bestrahlung wurde dabei in situ mit ESR verfolgt. An Hand der Spektren und der Intensitäten sowie der eintretenden Änderungen während der UV-Bestrahlung konnten eindeutig Unterschiede in der Stabilisierung der LDPE-Folien nach wenigen Minuten bzw. Stunden Bestrahlungszeit identifiziert werden. So gelang es, ein Ranking von LDPE-Proben nach der Stabilisatorkonzentration aufzustellen, wie auch nach der Wirksamkeit unterschiedlicher Stabilisatortypen (bei jeweils gleicher Konzentration). Diese Ranglisten standen in sehr guter Übereinstimmung zu den bei der künstlichen Bewitterung ermittelten. Vorteil dieses Verfahrens ist, dass die Wirksamkeit von Stabilisatoren nach wenigen Stunden Belichtungszeit festgestellt werden kann. Es ist denkbar, durch spezielle ESR-Zellen nicht nur die In-situ-Messungen bei simultaner UV-Bestrahlung zu messen, sondern auch bei Plasmabehandlung. Es ist ebenfalls vorstellbar, daß die Bedingungen der künstlichen Alterung in einer speziellen ESR-Zelle mit Temperatur- und Druckbeaufschlagung sowie breitbandiger UV-A-Bestrahlung realisiert werden können. In einem solchen Falle könnten

neu entwickelten Materialien, neue Stabilisiatorentwicklungen und –kombinationen innerhalb weniger Stunden getestet werden.

1. Introduction

In the past few decades, the polymer manufacturing has been increasing at a very rapid pace and development of new polymer composites has also gone up. Statistics show that more than half of the polymers produced are extensively used in outdoors. The global consumption of polyethylene in 2010 was about ~70 million metric tons and the demand will be in this trend for the next ten years. In 2010, High density PE (HDPE) accounted for around 45% of global polyethylene consumption, followed by linear low density PE (LLDPE) and low density PE (LDPE) as shown in Figure 1 [1]. Over a half of LDPE is used for film/sheet applications and the majority of greenhouse areas are covered by LDPE films [2].

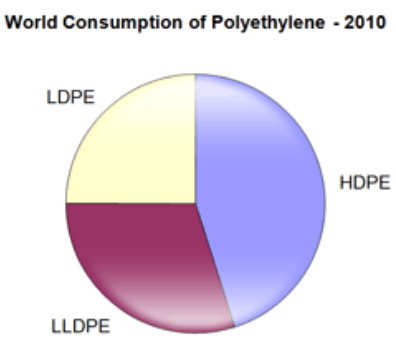

Figure 1: Pie chart of global consumption of polyethylene in 2010.

LDPEs which are extensively used in outdoor applications are exposed to solar UV radiation (290-400 nm) and one of the main factors that affect the polymer efficiency is their instability towards photo-chemical reactions [3]. Despite solar UV radiation other factors such as temperature, air, pollution, and physical stress play a significant role in the degradation of polymers. In addition, there is a practice of underestimating other environmental agents, such as water (in form of moisture, snow, rain, fog, dew and frost), which also play an important part in the degradation process in almost all polymers [4]. Once the stage of mechanical disintegration is reached, the materials become useless and have to be disposed. In practice, these broken films are considered as waste and dumped in unauthorized areas posing a great threat to the environment. Hence producing polymer films that have longer durability become

absolute necessary. In this context the study of photo-degradation of LDPE is vital owing to its scientific, industrial and environmental importance [2].

1.1. Scopes and objectives

The study was performed in LDPE considering its importance in the day-to-day life. Even though it is a widely studied topic for decades, still the photo-physical and photo-chemical processes at the surface and the bulk remain a subject of discussion. In this note, it is important to evaluate the pathway to degradation and mainly, understand the surface and bulk property changes of the polymer. Thus, to improve the longevity of polymer lifetime, the understanding of reaction mechanisms involved in photo-degradation is necessary. Much of the discussion focuses on the effects of UV, as this is considered to be the main weathering factor that hinders the performance of any polymer.

The work is aimed at understanding the effects of photo-oxidation in LDPE induced by few testing methods and analyzing at periodic intervals. In order to realize this aim, following objectives has to be achieved:

- To simulate the effects of solar UV with varied humidity using artificial weathering device and study the effect of photo-oxidation through surface and bulk analysis.
- To explore oxygen plasma weathering at a relatively shorter time (in hour) to check for any correlation with the effects of artificial weathering.
- To investigate the nature of photo-oxidation by exposing the LDPE to bromine vapor after argon plasma.
- To study the degradation profile of LDPE at relatively shorter times using UV in-situ weathering of HALS-stabilized and unstabilized LDPE with ESR measurement.

1.2. Thesis overview

This dissertation has been divided into following chapters: Chapter 2 discusses the scientific background related to weathering effects of LDPE. Chapter 3 details the different techniques that are employed to study the effects of weathering and Chapter 4 deals with results and discussion. Finally ends with conclusion in Chapter 5. An overview of the methods, analytical techniques used and the presumable mechanisms that are extensively used in this work are briefly summarized below:

Testing methods	**Exposure time**	**Analytical technique used**	**Mechanisms involved**
Weathering device	in days	XPS, FTIR-ATR, DRS, DSC, Tensile strength	oxidation via chromophores and a few radicals, presence of humidity, time-consuming
Oxygen plasma & Effect on surface photo-oxidation after Br vapor	1- 5 h	XPS, FTIR-ATR, tensile strength, UV-Vis	fast scission of C-C- and C-H-bonds, formation of C=C and polyenes, oxidation of radicals and double bonds, absence of humidity, absence of oxygen diffusion into the polymer, shielding of UV by polyenes, very high acceleration
UV-A in-situ irradiation	1- 6 h	ESR	oxidation via chromophores and radicals, absence of humidity

Analytical methods	**Sampling depth**	**Information obtained**
XPS / ESCA	0.001- 0.01 µm	elemental composition, oxidation state
FTIR-ATR (diamond cell)	2.5 µm	functional groups (oxidation)
UV-vis	several millimeters	C=C bonds, oxidation
DRS	several millimeters	degradation, crosslinking, oxidation
ESR	several millimeters	radicals, chain scission
Tensile strength	several millimeters	mechanical strength, ageing

2. Degradation and photo-oxidation of LDPE

2.1 Principle of degradation

"The amount of energy absorbed by a molecule must exceed the bond energy to cause degradation" [4]

A useful weathering study has to obey this principle of degradation for two main reasons:

1. Energy must be absorbed by a molecule for it to make any changes in molecular structure.
2. A change in the energy of radiation source will affect weathering.

One has to take extreme care in choosing the type of radiation for the following reasons:

1. The shorter the wavelength the larger the energy of radiation
2. Visible light and infra-red radiation are transferred has heat during photo-chemical processes
3. UV-A, B and C and vacuum UV have sufficient energies for $\pi \rightarrow \pi^*$ transitions associated with scissions of covalent bonds
4. X-rays and γ-rays have higher energy than solar radiation and hence the results cannot be compared [4].

2.2. UV induced photo-oxidation in polymer

Solar radiation spectrum ranges over 290-3000 nm and it consists of just less than 10% of UV radiation but it has sufficient energies to dissociate C-C or C-H bonds in polymer. The free radicals produced in this way may then react freely with the atmospheric oxygen and contribute to further degradation of the polymer, which is called photo-oxidation. The polymer ability to resist solar UV is mainly affected by the presence of impurities or chromophores. Such chromophores (catalyst residues, carbonyl groups, double bonds) can absorb UV radiation and initiate the photo-oxidation reaction. In natural ageing process the

combination of solar UV in the presence of oxygen in air can produce irreversible damage to the polymer. The pathway by which an organic material (RH) undergoes auto-oxidation process takes place in four steps [5-8]. In initiation, the free radicals are produced through energy transfer in the polymer and the incident UV radiation. These free radicals react with oxygen to give away hydroperoxide radicals which on reacting with hydrogen to form hydroperoxides in the propagation. The hydroperoxide radical can also react with another alkyl radical to produce hydroperoxides and a radical.

1. Initiation:

$$RH \rightarrow Free\ radicals, ex.,\ R\bullet,\ H\bullet$$

2. Propagation:

$$R\bullet + O_2 \rightarrow ROO\bullet$$

$$ROO\bullet + RH \rightarrow ROOH + R\bullet$$

3. Branching:

$$ROOH \rightarrow RO\bullet + OH\bullet$$

4. Termination:

$$ROO\bullet + ROO\bullet \rightarrow ROOR + O_2$$

$$R\bullet + R\bullet \rightarrow R - R$$

$$RO\bullet + H\bullet \rightarrow ROH$$

$$R\bullet + H\bullet \rightarrow RH$$

Further, the hydroperoxides can dissociate into alkoxy and hydroxyl group in branching. Finally, when two radicals react together then termination occurs by forming cross-linked polymer, short chains and hydroperoxides [5-8].

2.3. Photo-oxidation mechanism of LDPE

PE has the known general formula: $(C_2H_4)_n$ and a semi-crystalline polymer. LDPE has a long chain with 5-10 short branches per 1000 C atoms. The density of LDPE is of the range 0.91-0.93 g/cm³ and the crystallinity between 42-53% [3].

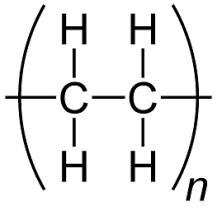

In the past, extensive research has been done on the photo-degradation of polyethylene [9-22]. Theoretically, LDPE should be photo-oxidatively stable due to its stable chemical structure. However, the presence of light absorbing chromophores imparts photosensitivity on the LDPE films [4,23].

The types of chromophores in polyolefins are widely debated. Few assume that hydroperoxides are light absorbing part in polypropylene [24] while it is understood that carbonyl groups are active chromophores in UV irradiated PE [22]. During photo-degradation two kinds of reaction occur predominantly: chain-scission and crosslinking [4]. When alkyl radicals react with one another subsequently neighboring linear chains can get linked to another by covalent bond formation called as crosslinking [25]. Whereas the termination step of photo-oxidation could lead to scission of long chains into shorter ones called as chain-scission. During photo-degradation chain-scission and /or cross-linking occur [10,12,17,26]. For example, copolymerization of an ethylene monomer with traces of carbon monoxide forms an ethylene-carbon monoxide copolymer, prone to degrade on solar UV exposure through Norrish type I and II mechanisms as shown in scheme 1 [3-4,9-10].

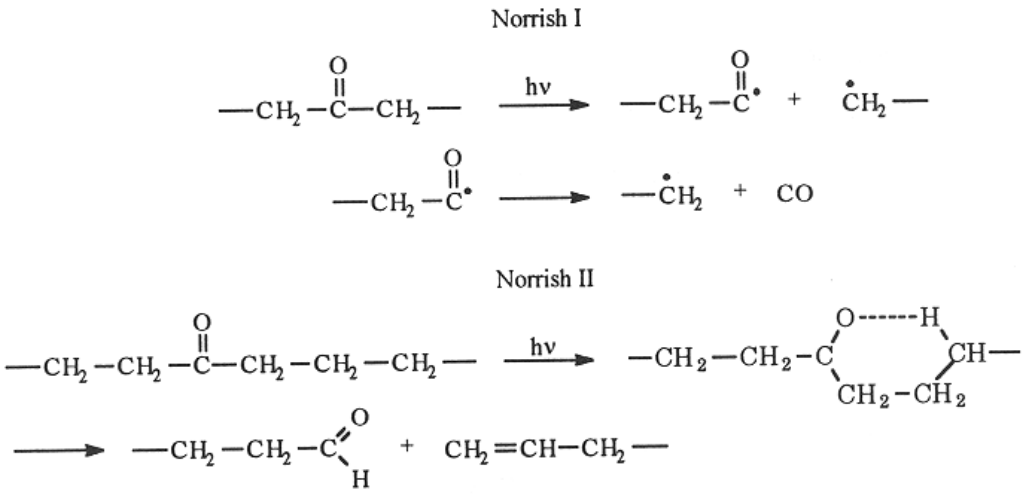

Scheme 1. Norrish I and II mechanisms of polyethylene.

Both mechanisms affect the longevity of the polyethylene to a larger extent. If the polymer degrades according to Norrish I mechanism, two free radicals are formed simultaneously. If the Norrish II mechanism dominates degradation, two molecules are formed which can absorb sunlight. These two mechanisms can result in a self-accelerated degradation process. The unsaturations formed in low-density PE are as follows:

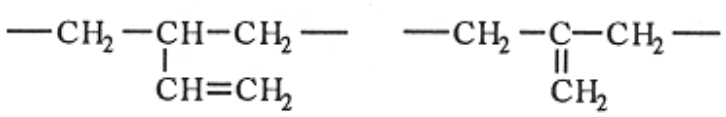

The presence of these unsaturations (vinyl or vinylidene groups) leads to formation of allylic hydroperoxides during the thermo-oxidative processes and this could be also an initiator:

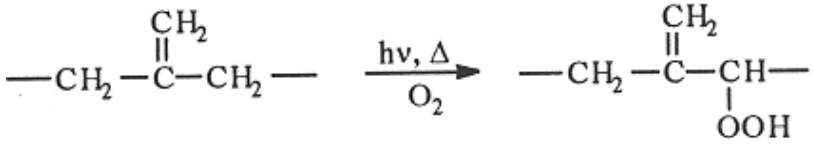

This structure can be degraded further by thermal energy, UV, or other radicals to free radicals and/or to structures containing UV-absorbing groups (e.g., carbonyl). Some research indicates that peroxide decomposition is limited to local conversion through a cage effect. This would assign a relatively restricted role to hydro-peroxide as the initiator of chain reactions because the radicals produced would react to form inert material (water) directly

after their formation. Chain scission reactions, as explained above, usually predominate, but crosslink formation also occurs:

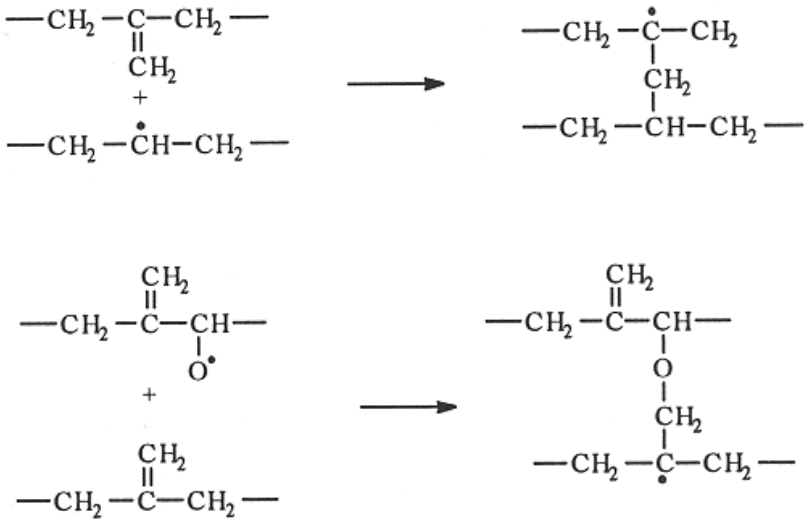

By the end of termination step long LDPE molecular chains degrade into several short chains [3].

2.4. Weathering

Weathering is a study of slow changes in the physical and chemical properties with dependence on time. Long term exposure tests can be a useful tool in understanding the photo-degradation process which helps in increasing the polymer service life time [10,13].

The most common testing methods are:

1. Natural or Outdoor weathering
2. Artificial weathering
    a. QUV fluorescent lamps
    b. Xenon arc lamps
    c. Mercury lamps

However a part of the present study deals with the effect of photo-oxidation induced by UV radiation from QUV fluorescent lamp. A brief overview of natural and artificial weathering of LDPE is given here.

Natural weathering of polyethylene

Natural weathering or outdoor weathering of polymer can be useful because of the combination of all weathering agents such as, sunlight, air, rain, dew, humidity, pollution etc., A standardized method has also been adopted keeping Florida as location with the samples vertically inclined at 45° facing south as shown in Figure 2 [27]. However, the main challenge in natural weathering is the reliability of data due to geographical locations, day/night temperature, varying seasons, pollution, etc.[28]

Figure 2: Polymer samples are stacked in the natural weathering field at South Florida [28].

The crucial role of temperature on the weathering of polyethylenes was illustrated on desert exposure of polyethylene films. The natural weathering study of LDPE and HDPE using ASTM 1435 D was undertaken and the energy needed to break chemical bonds of polymers of different kinds was calculated and it was correlated to the energy dissipated from the sun to the polymer matrix during the overall exposure period [29]. Mostly elongation at break was measured to demonstrate the extent of degradation by outdoor weathering [30]. The rate of weathering of commonly used polymers are much slower when they were exposed floating in sea water in marine environment than to those weathered on land [31].

A set of HDPEs were naturally weathered in Rio-de-Janeiro and it was noticed that there was a decrease in the molecular weight and around 40% decrease in the elongation-at break [32]. While weathered during Canadian winter, HDPEs show no significant change in the molecular weight and mechanical properties [33]. Suzuki et al. carried out outdoor weathering

test with HDPE and LDPE and noticed that within the first month of exposure, ultimate elongation increased slightly and then reduced [34]. The main disadvantage of outdoor weathering tests is the time-consumption. In the case of weathering of HALS or any stabilized polymers, it might take years to get results [10,13].

Artificial weathering

The necessity to evaluate the degradation mechanism more rapidly is the reason behind the choice of laboratory or artificial weathering. The advantage of artificial weathering is the leverage to manipulate the various weathering agents to an extent where it could be comparable to the actual effects. The other preferable advantage is the reproducibility and repeatability [28].

The most common artificial sources for UV radiations are the xenon arc and fluorescent lamps. It is a convention to call it as QUV tests, when fluorescent lamps are used [10]. The radiation spectrums of these two sources are in good agreement with the solar UV. However, the Xenon lamp contains wavelengths shorter than the cut-off levels of solar UV which makes usage of filters, a must. Also, the emission of IR at higher levels needs to be controlled to prevent over heating of the polymer. Nevertheless, fluorescent lamps are cost efficient and do not emit high energy IR. There are two types of fluorescent lamps: UV-B and UV-A. The intensity of UV-B is centered on 313 nm and has emission below the solar cut-off (270-295 nm). This enhances the acceleration and initiates unwanted reactions; whereas, UVA-340 do not have this problem and closely match the solar radiation up to 350 nm. The low level emissions of visible radiation and IR in UV-A, make it more preferable for weathering studies [13].

LDPEs are extensively used outdoors and require withstanding a range of climatic conditions. So, this requirement needs to be fulfilled through some testing devices which have control over the following parameters:

1. UV radiation
2. Humidity
3. Temperature
4. Rain (including acid rain)

Weathering tests in the current study were carried out in Global UV Test 200 (Weiss Umwelttechnik GmbH, Reiskirchen, Germany) fitted with fluorescent UV lamps in the wavelength range from 290 to 460 nm, which is based on the ISO 4892-3 as shown in Figure 3. A small disadvantage is the limited control over the influencing factors such as specimen temperature and humidity [35].

Figure 3: Picture of weathering chamber used in this work [35].

Figure 4 shows the spectral irradiance of the Global-UV test unit in comparison with the overall range of solar UV radiation [36].The total irradiance in the UV range corresponds to the maximum UV irradiance in Davos.

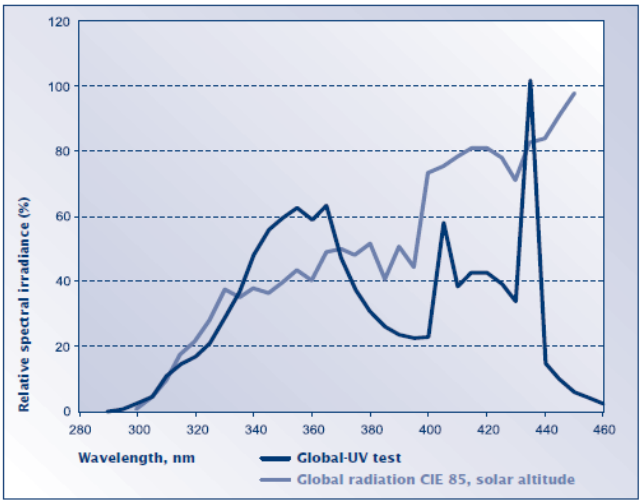

Figure 4: Spectral power distributions of fluorescent UVA-340 lamps and CIE solar light [35].

2.5. Understanding of artificial weathering through photo-oxidation of LDPE

The intensity of photo-oxidation can only be studied by using some analytical techniques. The two main indications of photo-oxidation are formation of new oxygen functional groups and change in the crystallinity due to cross-linking and or chain-scission. LDPE undergo similar oxidation pattern by the attack of free radicals on the polymer chain followed by reaction of the alkyl radicals with oxygen leading to various products such as hydroperoxides, alcohols, acids, ketones, esters, etc. [37]. For transparent PE films, photo-oxidation can only take place in the near-surface region, since the oxidation process is limited by the diffusion of oxygen inside the material [38]. Photo-oxidation produces surface crazing and fracture in polymers caused by chain scission and /or cross-linking. Not all polymers are equally affected by weathering; for instance, unstabilized LDPE film becomes completely brittle after only a few weeks of exposure. For PEs, both cross-linking and chain scission may take place simultaneously as a result of weathering [39].

FTIR

FTIR is commonly used to identify the changes in surface photo-oxidation in the polymer by determining the functional groups at surfaces. FTIR by attenuated total reflectance (ATR) is a method that does not alter the actual surface of the sample. It is a widely used technique and the working principle is detailed in [4].

Chemical bonds absorb UV photons of varying frequencies and different functional groups in the polymer can be detected by the absorption of IR at a particular frequency. Carbonyl groups (C=O) are formed after chain-scission and oxidation, which is an indicator of photo-oxidation. FTIR can be used to identify these carbonyl groups such as, ketones, carboxylic acids and aldehydes [4]. Based on FTIR, many studies have been reported on PE after weathering; by monitoring the carbonyl group, vinyl group (908 cm^{-1}) formations [4,8,20,22,30,37].

The presence of carbonyl group is seen as a broad peak at 1710 cm^{-1}. By deconvoluting it, following functional groups can be identified: Carboxylic acid (1700 cm^{-1}), Ketones (1714 cm^{-1}), Aldehyde (1733 cm^{-1}) and Esters (1733 cm^{-1}). To evaluate the effect of photo-oxidation, carbonyl index is measured. It is defined as the ratio of the band absorption in the carbonyl group at 1710 cm^{-1} to the absorbance of intense peak due to the asymmetric C-H stretching at 2924 cm^{-1} [40,15,22].

XPS

X-ray photoelectron spectroscopy has been used in this work because the photo-oxidation induced by accelerated weathering begins from the LDPE surface. The sampling depth of XPS is ~6 nm. The XPS principle is extensively discussed in [4,41]. By analyzing the XPS spectra following information could be extracted [41]:

1. Nature of impurities and the temporal evolution of oxygen on the surface which is critical in weathering studies

2. The chemical environment of carbon and oxygen can be studied by deconvolution of C1s or O1s spectra.

XPS has also been used to study the photo-oxidation of weathered PE in the past [42-48]. In a survey scan of oxidized PE, broadened C1s peak is centered at 285 eV and O1s peak at 532 eV indicating the oxidation. From the low resolution spectra, elemental oxygen to carbon ratio (O/C) can be determined. The types of O-C bonds can be determined by curve-fitting of C1s from high resolution spectra and can be found that C1s is a four component spectra with peaks centered around 285.0 eV, 286.5 eV, 288.7 eV and 289.3 eV. These four peaks correspond with C-C or C-H, C-OH or C-O-C, O-C-O or C=O and O-C=O respectively [4,41].

DRS

Dielectric relaxation spectroscopy is a sensitive tool to study the fundamental molecular motions and relaxation processes in the polymer. The working principle has been explained in detail in [56]. In the past there are studies that have been carried out to analyze the weathering effects of LDPE after gamma irradiation [49-53], while only a very few systematic studies have been carried out to explore the dielectric properties of UV weathered LDPE in air under dry conditions (less than 15% RH) [54,55].

A dielectric study of artificial UV weathering of LDPE benefits from the fact that neat LDPE is a non-polar polymer, upon UV irradiation radicals are generated by C-C and C-H bond scissions, which act as a probe for dielectric measurements [56]. Also a dielectric probe technique was employed used to study the molecular dynamics of polyolefins [57]. These radicals undergo either fast recombination or auto-oxidation via peroxy radical formation giving rise to carbonyl and/or keto groups etc. [58]. The dielectric response of pure polyethylene is quite low because there is no intrinsic dipole moment. The weak dielectric losses observed are due to the presence of impurities in PE. Moreover by oxidation processes a small number of polar carbonyl groups can be formed [59,60]. Titanium dioxide was incorporated to control the oxidation without appreciable change in crystallinity [61].

Since polyethylene is a semi-crystalline polymer and often classified as two-phase systems i.e. crystalline and amorphous region. The chain-scission and or cross-linking occur

predominantly in the amorphous regions because oxygen can diffuse through such regions relatively freely when compared to the tightly packed crystalline regions [17].

Chain scission leaves shorter chain segments that were previously entangled and allows them to crystallize. When these shorter segments are available enough to crystallize, new crystals could form but it is more likely that these segments will attach to the growth faces of pre-existing crystals nearby. This will increase crystallinity and is a form of secondary crystallization often known as "chemi-crystallization" [10,12]. Increase in crystallinity and embrittlement is manifested by replacing C-H bonds by C=O bonds in LDPE [62].

The dielectric mechanism is directly connected to molecular fluctuations in the polymer which can be seen in the different relaxation processes. Polyethylene shows three dielectric relaxation processes, called the α_c-, the β-, and the γ-relaxation.The α_c-relaxation is due to the molecular fluctuations in the crystalline regions and occurs at lowest frequency or higher temperatures. Its molecular nature is still under discussion. A rotational-translation of chain segments assisted by a chain twisting is discussed as a mechanism [63,64,65]. The β-relaxation process is related to segmental motions in the amorphous phase responsible for the glass transition. Therefore this process is also called dynamic glass transition (It is worth to note that for amorphous polymers this process is called α_c relaxation [57]). The β relaxation is observed at higher frequencies or lower temperatures than the α_c-relaxation. At the lowest temperatures or highest frequencies the γ relaxation takes place which corresponds to localized fluctuations in the amorphous region of the polymer [56,66].

Part of this work deals with the dependence of the above mentioned dielectric processes of LDPE on UV weathering and discusses how dielectric spectroscopy could be used to understand the mechanical disintegration due to artificial weathering. The dependence of activation energies and dielectric strengths of the α_c and β relaxation processes on the weathering time is also discussed in detail. It is noticed that dielectric relaxation spectroscopy could be a viable tool to analyze the effects of artificial weathering [54,55,67].

2.6. Plasma weathering of polymers

There have been only fewer studies on plasma weathering of polymers [68-72]. The ageing of plasma polymers, post-plasma ageing and surface modification of polymers are widely researched. Plasma irradiation is very fast and high acceleration of degradation is possible and hence classified as "ultra-accelerated artificial aging" [73]. To realize the ageing effects in the polymer bulk several hours of plasma treatment is required. Interestingly, the effects of artificial, outdoor, photo-oxidation, thermal ageing of polymers are similar to those exposed to plasma irradiation for longer hours [74] while, the reactions under plasma irradiation are quite different from those prevalent during weathering [75]. Few researchers have found a correlation of oxygen plasma weathering of PET with outdoor weathering and Xenotest. The tensile strength of PET shows good agreement when weathered naturally and Xenotest in comparison with oxygen plasma weathering. The acceleration factor for oxygen plasma irradiated PET to natural weathering was around 350 [70]. Another study was made on polypropylene and it was found that there was a loss of 60% in elongation at break for 10 s oxygen plasma treatment in comparison with natural weathering [72]. Influenced by these developments, LDPE was treated with oxygen plasma for longer time periods (hour) to check for any correlation with the weathering effects.

If a polymer is treated under plasma, UV photons with wavelength shorter than about 200 nm can attack the chemical bonds in polymer without the need of any chromophore. These energies exceed the dissociation energies of all covalent bonds in polyolefins (3.5-3.7 eV). The scission of C−C (~3.5 eV) and C−H (3.5-4.0 eV) in polyolefins by $\sigma \rightarrow \sigma^*$ transitions are induced by plasma vacuum UV radiation. Since C-C and C-H dissociation energies are similar and therefore the probability of C-H and C-C bond scissions is nearly equal. When polymers are exposed to the oxygen plasma its vacuum UV radiation induces H-abstraction, chain scission and therefore generation of free radicals which can form new species through auto-oxidation. The auto-oxidation reaction takes place with the presence of C-radicals as described below:

$R\bullet + \bullet O\text{-}O\bullet \rightarrow R\text{-}O\text{-}O\bullet$

$R\text{-}O\text{-}O\bullet + R'H \rightarrow R\text{-}O\text{-}OH + R\bullet$

$R\text{-}O\text{-}OH \rightarrow$ *decay or rearrangement to different products*

In turn, auto-oxidation introduces peroxy radicals (R-C-O-O•) by reaction of molecular oxygen with C-radicals, which were converted to hydroperoxides (R-O-OH) followed by formation of peroxides ($R^1O\text{-}OR^2$) or more probable by decay and rearrangement to alcohols, ethers, epoxides, ketones (R^1R^2CO), aldehydes (CHO), carboxyl (RCOOH), esters (R^1COOR^2) and peroxy acids (R(O)-O-OH) and these oxygen containing functional groups can be studied by XPS and FTIR [4,74].

Plasma surface modification

LDPE surface can be modified by using low pressure plasma depending upon the requirements for different applications. Usually post plasma treatments with Br or NO gas has been done to label the radicals that are formed after plasma irradiation. The plasma generated radicals can be quenched using radical scavengers like 2,2-diphenyl-1-picrylhydrazyl (DPPH) or 2,2,6,6-tetramethylpiperidine-*N*-oxide (TEMPO) through liquid phase reactions [76, 77]. NO (or NO_2) gas can also be used as radical scavenger. Primary carbon radicals are expected to form nitride groups, secondary radicals form oxide groups, and tertiary radicals nitro so groups [78,79]. The N 1s peaks of UV-irradiated polyethylene or isotactic polypropylene could be fitted into four components at 400.5, 403.7, 406.2, and 408.1 eV, which were assigned to oximes, nitroso, nitro groups, and nitrates. The origin of all these nitrogen containing functional groups was explained as follows. Primary and secondary radicals react with nitric oxide forming nitroso groups, which are immediately transformed into oxime groups via nitroso-oxime tautomerism. Tertiary radicals form nitroso groups, which cannot tautomerize because of absence of H bonding with carbon atom. These nitroso groups, however, can react with further nitric oxide to nitro and nitrate groups [80].

NO is also able to abstract hydrogen atoms from hydroxyl groups in an oxygen free environment. Thus, alkoxy radicals are formed (R-OH + •NO → R-O• + NHO). Nitrates are

formed by the reaction of NO with peroxy or hydroperoxy radicals, and a reaction with an alkyl radical yields a nitroso group. Such nitrogen functional groups were identified by XPS. It was found that the total nitrogen concentration is equal to the number of radicals formed and also the type of radicals [79].

Plasma bromination of polyolefins has been tried by many researchers to modify the surface [81-85]. Such polyolefin bromination has the character of a plasma-assisted substitution reaction [85]:

$$Br_2 + plasma \rightarrow 2 \bullet Br$$

$$R - H + \bullet Br \rightarrow R \bullet + HBr$$

$$R \bullet + \bullet Br \rightarrow R - Br$$

In contrast to the previous studies, the current work deals in investigating the nature of photo-oxidation process by introducing bromine in gas phase immediately after argon plasma treatment of LDPE.

2.7. Stabilization of LDPE

It is known that LDPE is vulnerable to UV radiation, to increase the durability few stabilizers have been developed to hinder or slow down the degradation upon UV exposure. The two main types of photostabilizers are UV absorbers (UVA) and hindered amine light stabilizers (HALS). Sometimes, pigments are also used to inhibit photo-degradation. The main pre-condition of stabilizers is to absorb UV light before the polymer is affected [86,87]. An optimal photo-stabilization depends on the thickness of the sample [23].

Ultraviolet absorbers

UV absorbers are derivatives of benzotriazole and benzophenones as shown in scheme 2. As the name indicates, these compounds can absorb UV radiation and has the character of regenerating on its own and returning to their original form after the reaction [10,23].

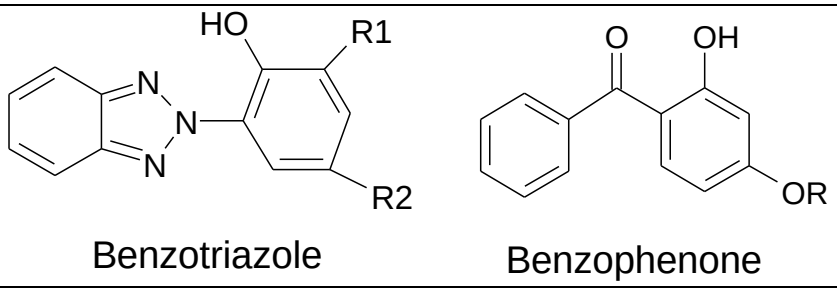

Scheme 2. Benzotriazole and benzophenone chemical structures.

Typical UV absorption spectra of benzotriazoles are shown in Figure 5. The absorption curves show that there is a strong absorption in the UV range between 250 and 425 nm and a large reduction in absorption in the visible range above 375 nm.

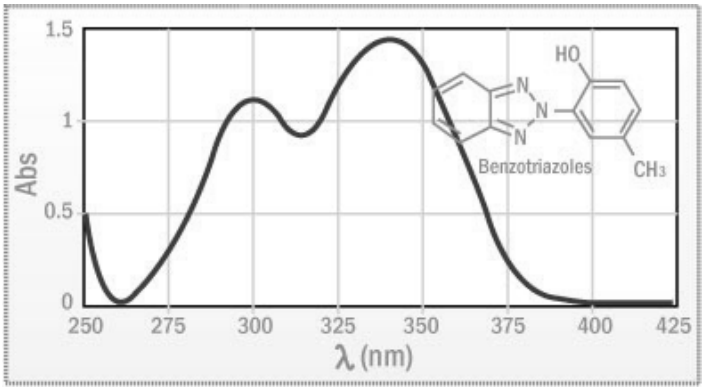

Figure 5: UV absorption of benzotriazoles. Source: [88].

The working mechanism of benzotriazoles is shown is scheme 3. UV absorption causes the electron density to move from the phenolic oxygen to the nitrogen atom. As a result, the nitrogen becomes more alkaline than the oxygen and a proton transfer occurs. This mesomeric form represents an excited state, which returns to the ground state with radiationless transition in the form of heat [13].

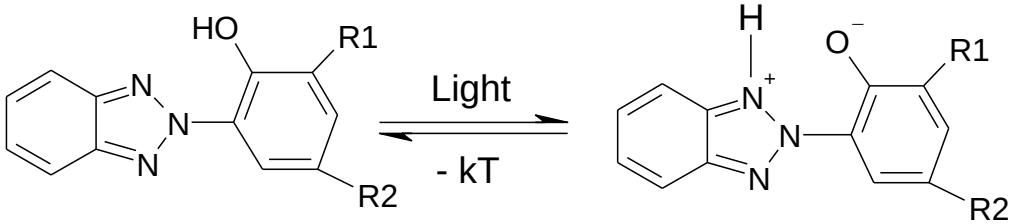

Scheme 3. The mechanism of hydroxyphenylbenzotriazole.

Hindered amine light stabilizers (HALS)

HALS are derivatives of 2,2,6,6-tetramethyl piperidine (Scheme 4) and are extremely efficient stabilizers against light-induced degradation of most polymers. Unlike UV absorbers, HALS does not absorb UV radiation, but act to inhibit degradation of the polymer.

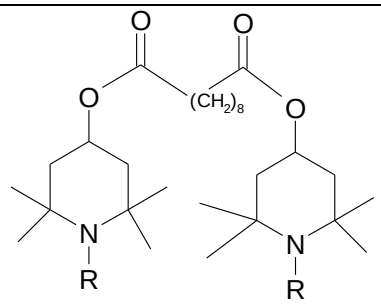

R = H, CH_3 or OC_8H_{17}

Scheme 4. Structure of 2,2,6,6-tetramethyl piperidine.

A major advantage of HALS is that no specific layer thickness or concentration limits needs to be reached to guarantee good results. Significant levels of stabilization are achieved at relatively low concentrations. HALS's high efficiency and longevity are due to a cyclic process, wherein the HALS are regenerated rather than consumed during the stabilization process.

The mechanism of HALS against thermo-oxidation appears to be complex. Because of the regenerative nature of this process, as well as the typically high molecular weights of the stabilizers, HALS are capable of providing extreme long-term thermal and light stability.

Still there is a continued research is on the working mechanism of HALS [89,90]. To understand the action mechanism of HALS, Haillant and Lemaire came up with a scheme as shown in Figure 6 [91]. HALS is able to form a nitroxyl radical which decreases the amount of oxygen available to degrade the polymer. Moreover, the nitroxyl radicals are stable and will not remove hydrogen from the polymer chain, yet it will react with another radical in termination reaction which de-activates the free radicals and breaks the chain reaction [10].

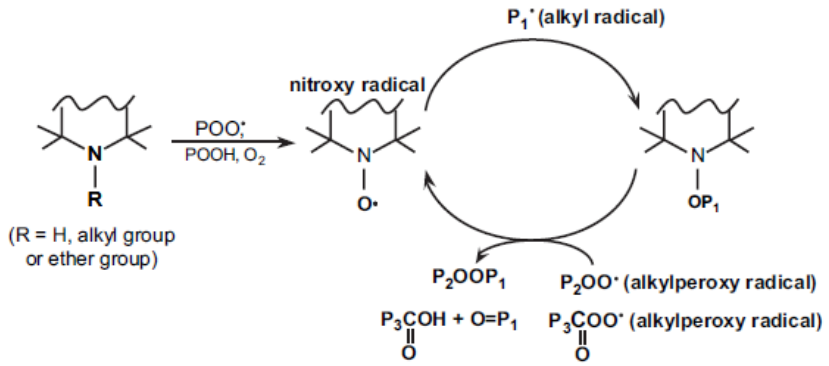

Figure 6: Working mechanism of hydroperoxide radical in HALS as explained in [91].

There are many studies reported on the weathering of HALS stabilized polyolefins [92-97]. Gijsman and Dozeman found a correlation between elongation at break and oxygen uptake in the UV weathering of HALS stabilized PE and neat PE. The oxygen uptake for HALS stabilized PE (1440 mmol/kg) is higher than the neat PE (920 mmol/kg) causing a difference of up to 50% in elongation at break. Neat PE lost nearly 50% of its tensile strength after 7 months of outdoor weathering in Florida, whereas with HALS stabilization, the same 50% was reached after 5 years of exposure [23]. HALS stabilized greenhouse films were shown to last 33% longer than Ni stabilized in testing under real conditions and being sprayed with a variety of agrochemicals. It should also be noted that HALS additives act also as heat stabilizers and minimize the effect of high temperatures [2]. HALS shows good resistance to UV radiation, whereas hydrolytic ageing of HALS is not very effective [47,48].

3. Experimental

3.1. Artificial weathering tests

Inside the weathering chamber, the spectral distribution characterized by UVA-340 nm lamps (type 1A, A.1 of ISO 4892-3, table 1) were enclosed within PVDF membrane. The PVDF membrane in the weathering device has more than 95% of UV transmission. Since the spectral distribution is limited to UV and near VIS, radiation heating can be neglected ($T_{Surface}–T_{Chamber} < 2K$).

The measured UV irradiance of the lamps with wavelengths ranging from 290 to 400 nm was 45 Wm^{-2}. The UV radiant exposure is defined as the time integral of irradiance. For example, if the weathering intervals are 3, 6, 12, 25, and 32 days then the corresponding radiant exposure are 12, 23, 47, 97, and 124 MJm^{-2} respectively. The experiments were done under varied relative humidity at 60 $^{\circ}C$. The samples which are weathered under dry conditions (<15% RH) are placed directly in the chamber (Figure 7) and for samples at >90% RH a special water-proof box was made to place within the device as shown in Figure 7. Because of the PVDF film cover of the box, the irradiance is approximately 20% less than that for the sample weathered under dry condition. For example, 81 days of UV weathering with radiant exposure of 325 MJ/m^2 is roughly comparable with 1 year outdoor exposure in Phoenix (Arizona) or in Northern Australia.

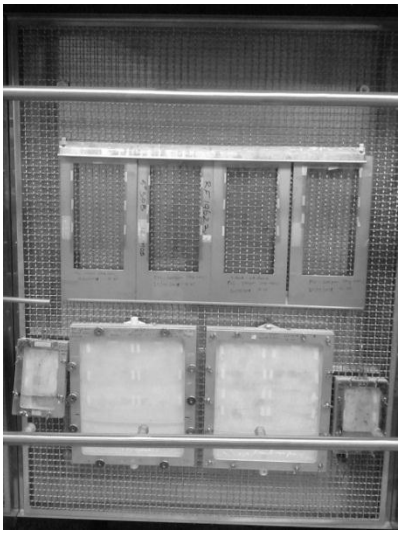

Figure 7: LDPE films that are loaded in the chamber for dry and humid weathering.

3.2. Plasma weathering

A model experimental set up used for the oxygen plasma weathering is shown in the Figure 8. Here, the plasma geometry is shown as rectangular frame for better understanding. The reactor used in the work is cylindrical in shape.

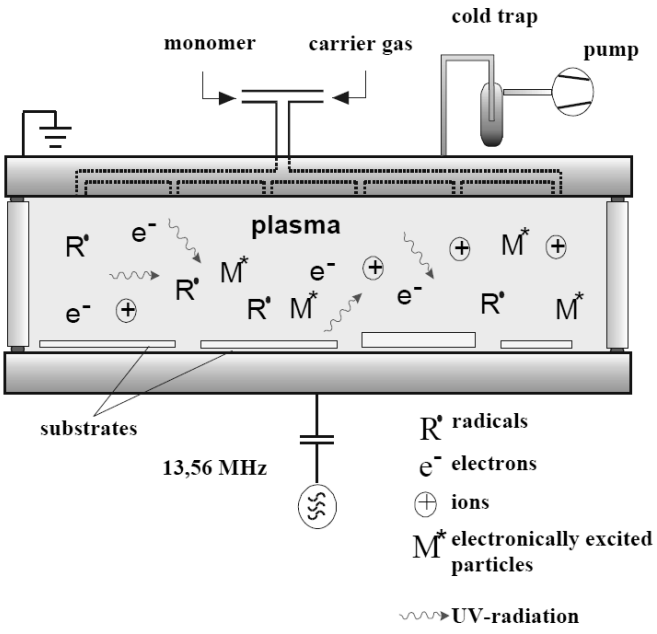

Figure 8: Model plasma chamber and its components [98].

Plasma chamber

The Figure 8 shows the plasma reactor and its parts. The cylindrical plasma chamber was made of stainless steel and has a diameter of 15 cm. The two electrodes are diode-like arranged within the reactor with a distance of 10 cm. The flow of the main precursor oxygen was controlled by a mass flow controller (MKS, Munich). The residual pressure before each measurement was found to be around 0.03 Pa. The plasma was ignited by means of 13.56 MHz radio-frequency source connected to the two electrodes through a matching network to reduce the reflected power. The oxygen pressure was 10 Pa and the operating power was chosen as 50 W because for prolonged weathering beyond 2 h, the heat generated inside the chamber should not melt the PE foils that are in use.

3.3. Materials

For the weathering studies, the UV-unstabilized and additive free LDPE films are commercial polymer from Goodfellow GmbH, Germany. They were used as supplied. The films are of semi-crystallinity in nature (50%) and 40 µm thick. The density of the films was around 0.92 g cm^{-3}.

For the plasma experiments, the same PE foils were used. The foils were cleaned with ether for 15 min in the ultrasonic bath to remove any impurities.

For radical quenching, liquid bromine (purity ≥ 99.5%, Merck, Germany) was used. To remove moisture and air in Br, it was degassed by freezing and evacuated to ca. 10^{-2} Pa for three times before using it. To realize a constant Br vapor it was stirred continuously using a magnetic stirrer.

The stabilized LDPE foils with 0.2, 0.8, and 1.0 wt% Hostavin N30 a light stabilizer belonging to oligomeric HALS class supplied by Clariant, Germany. The films are of 200 µm thicknesses. The materials were irradiated and were not subjected to any kind of pre-treatments.

3.4. Analytical techniques

XPS

The XPS analysis was described in detail elsewhere [85]. The sampling depth of XPS is about 6 nm. The XPS data acquisition was performed with a SAGE 150 Spectrometer (Specs, Berlin, Germany) fitted with a hemispherical analyzer Phoibos 100 MCD-5 and using non-monochromatic MgK_α or AlK_α radiation with 11 kV and 220 W settings at a pressure $\approx 1\times10^{-7}$ Pa in the analysis chamber. The angle between the axis of X-ray source and analyzer lens was 54.9°. The analyzer was mounted at 18° to the surface normal. XPS spectra were acquired in the constant analyzer energy (CAE) mode. The analyzed surface area was about 5×4 mm. The measured elemental concentrations were referenced to 100 C atoms.

FTIR-ATR spectroscopy

The FT-IR spectra were recorded with a NEXUS instrument (Nicolet, USA) using the ATR mode. The diamond cell, smoothing and base line corrections were done after the spectra were measured. The spectra were taken with 64 scans from the region 4500 to 550 cm^{-1} at a resolution of 4 cm^{-1}. The accumulated spectra give information in the surface-near layer of the polymer film of about 2.5 μm.

DRS

The weathered LDPE sample were placed between two parallel gold plated stainless steel electrodes of the sample holder of a high resolution ALPHA analyzer (Novocontrol) to measure the complex dielectric function $\varepsilon^*(f) = \varepsilon'(f) - i\varepsilon''(f)$. Here f is frequency, ε' the real part and ε'' the imaginary part or dielectric loss where i = √-1. The experiments were conducted isothermally in the frequency range from 0.1 Hz to 10^6 Hz. The temperature was increased from 173 to 413 K in steps of 2 K controlled by a Quatro Novocontrol cryo-system with temperature stability better than 0.1 K.

UV-vis spectroscopy

UV–vis absorption spectra was measured by means of a Varian UV Spectrometer Cary 300 (Varian Optical Spectroscopy Instruments, Mulgrave, Victoria, Australia), using an integrating sphere Labsphere DRA-CA-30I. The spectra were recorded in a double beam mode in the wavelength range from 850 to 220 nm.

Differential scanning calorimetry (DSC)

DSC measurements were done with a DSC 220C from Seiko instruments. The weathered LDPE samples were measured from 173 to 473 K with a heating and cooling rate of 10 K/min using nitrogen as protection gas. The enthalpy changes related to melting were calculated from 223 to 403 K.

Micro-tensile studies

The mechanical properties like Young's modulus and elongation at break (%) of weathered LDPE films were determined using an in-house made testing machine having a 5 kN load cell. It was operated at a speed of 150 mm min^{-1} with the grip distance of 80 mm on the film samples.

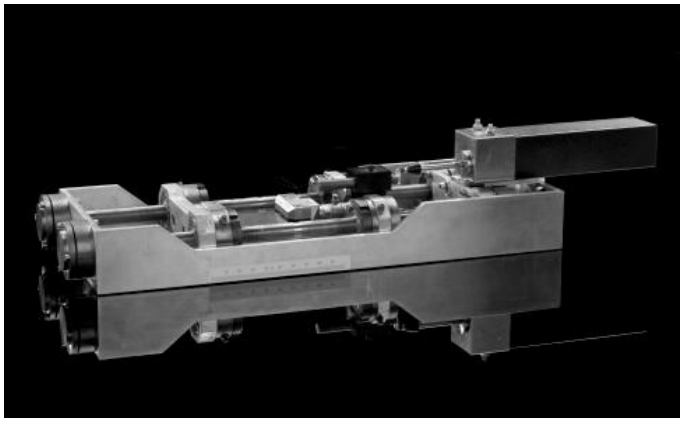

Electron spin resonance (ESR) spectroscopy

The ESR measurements were performed using a MiniScope MS-300 X-band spectrometer (9.3 GHz) with 100 kHz field modulation from Magnettech GmbH, Germany. To achieve in-situ UV irradiation, an ozone free mercury-xenon UV lamp from Hamamatsu, Japan (type L

8251-01) guided by light guide adaptor was fixed to the ESR spectrometer. The applied power was 200 W and the UV irradiance was 400 mW cm^{-2} at the sample position. The wavelength range of 300-450 nm was almost in the same range of sunlight that reaches the earth. The distance of the sample holder from the source lamp was 41 mm. All measurements were done simultaneously when the LDPE foils were irradiated continuously at room temperature under atmospheric pressure.

The ESR spectra were recorded with a sweep of 13 G/s (30 s sweep time at 400 G sweep width) and with a modulation amplitude of 4000 mG. The logarithmic plot of the microwave power versus the signal peak-to-peak height, a power level of 11 dB, which corresponds to 8 mW, was chosen in order to avoid saturation of the spin system. The modulation amplitude was adjusted to be less than half of the ESR signal line width to avoid artifacts in the spectra. The relative intensity was calculated by double integration of the recorded spectra.

4. Results and discussion

4.1. Artificial weathering of LDPE at 60°C with <15% RH and > 90% RH

Surface analysis

ATR-FTIR results

The FTIR spectrum in the ATR mode for additive free and non-oxidized PE is shown in Figure 9. The experimental conditions are same as mentioned in Chapter 3.4. The absence of C=O stretching absorption band at 1750-1680 cm^{-1} is an indication for absence of any photo-degradation. The most intense peaks are the methylene asymmetric and symmetric C-H stretching vibrations near 2920 and 2850 cm^{-1} and also the C-H bending vibration is seen near 1390 cm^{-1}.

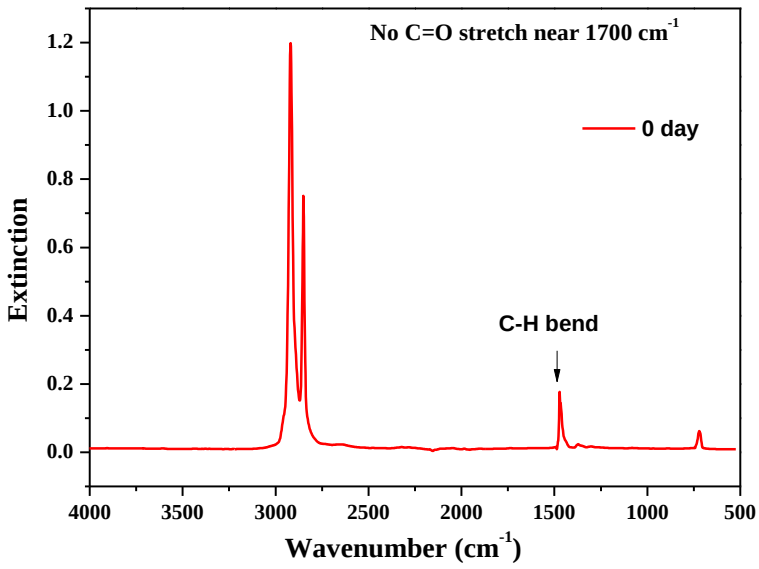

Figure 9: ATR-FTIR spectrum of an unweathered LDPE

When the same LDPE foil was weathered, one could see changes in the FTIR spectra as shown in Figure 10. The chain scission could be the reason behind the decrease in intensity of the C-H stretching and bending vibrations near 2900 and 1470 cm^{-1} respectively. The

carbonyl (CO) and hydroperoxide (OOH) frequencies are the best way to identify the effect of photo-oxidation of generated radicals. The absorption in the region 1200-1000 cm^{-1} could be due to the C-O stretching vibration and it could be interpreted as esters, carboxylic acids and ethers which absorb strongly in the region 1200-1000 cm^{-1}.

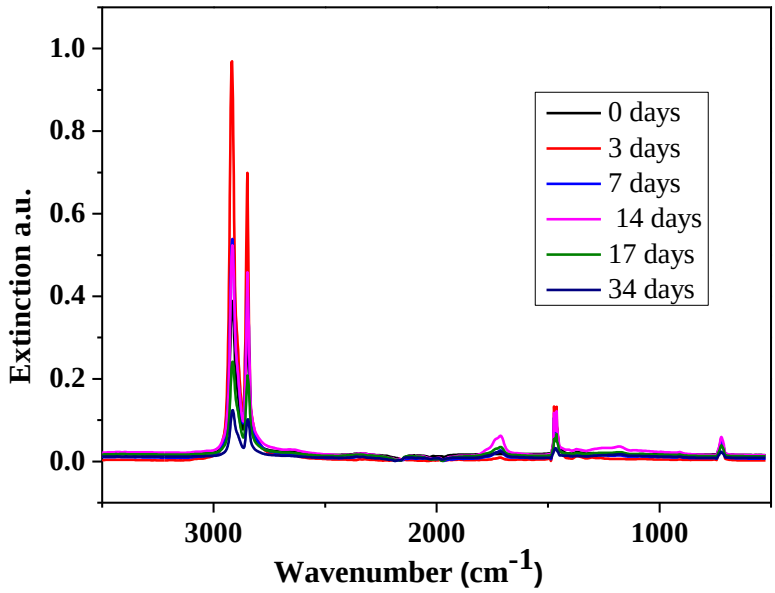

Figure 10: The FTIR spectra for weathered LDPE at different exposures.

Further investigations into the carbonyl groups can give certain vital information. The strong absorption in the region 1725-1705 cm^{-1} could be due to aliphatic ketone groups. The C=O vibrations of aliphatic aldehydes have absorption at 1730-1725 cm^{-1}.The aldehyde groups absorb at frequencies ~10 cm^{-1} higher than the corresponding ketone groups. But the carboxylic acid groups have absorption at 1760-1740 cm^{-1}. However, the hydrogen bonding can shift the absorptions toward 1725-1700 cm^{-1}. Figure 11 shows the dependence of carbonyl index C=O on exposure time derived from the region of 1820-1650 cm^{-1} which is normalized to C-H stretching vibration at 2921 ($\nu_{as}CH_2$) and 2850 cm^{-1} ($\nu_{s}CH_2$). The carbonyl groups could be assigned to aldehydes, ketones, carboxylic acids, esters etc.

The degree of photo-oxidation is seen as an increase of C=O absorbance versus the weathering period. In the case of <15% RH, the LDPE foil could not be weathered beyond 32

days and on the other hand with >90% RH the foils could not last beyond 15 days. The difference in the durability arises from the increased effect of humidity in the polymer. It was observed that the foil turned too brittle and finally disintegrated into pieces. The reason behind this behavior of the foil shall be discussed in detail in the next section.

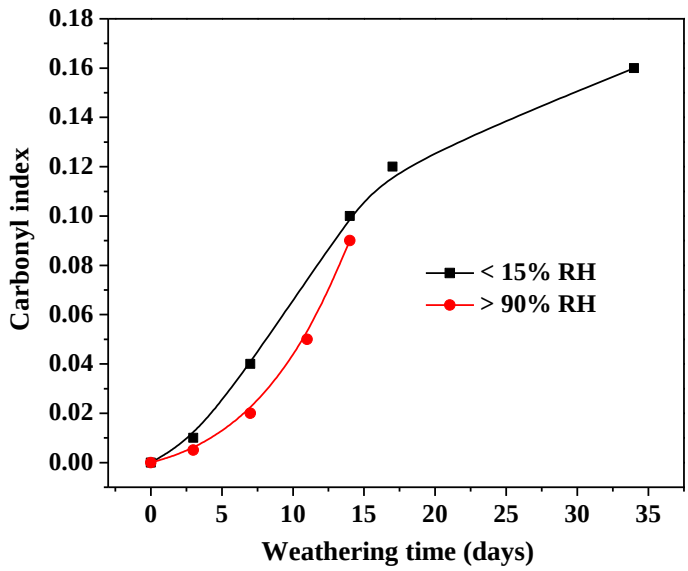

Figure 11: Carbonyl band (C=O) absorption normalized to C-H stretching vibrations against weathering time periods (days).

XPS results

The photo-oxidation at polymer surface can be analyzed by XPS and the experimental settings that are used in this study are explained in Chapter 3.4. The basic information such as O1s / C1s peak intensity ratio shows how the polymer oxidation proceeds during weathering. The deconvolution of the XPS core level bands gives the average binding energies for different products in detail. The core level XPS spectra for a neat PE foil (Figure 12) have only one strong peak at 285 eV due to the $–CH_2-CH_2-$ bonds in the polymer. The presence of oxygen in low levels is seen as O1s signal around 532-533 eV which is due to polymer processing and/or could be also due to the effect of storage. However, this O peak intensifies with those of the new produced $C-O_x$ species in the C1s peak.

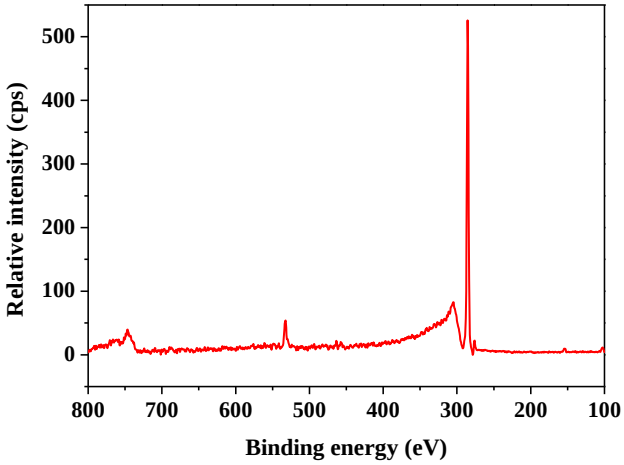

Figure 12: The core XPS spectra of a neat LDPE.

The Figure 13 shows the variation of O/C as a function of weathering period in days at <15% and >90% RH. The ratio of elemental O/C was determined from the low-resolution spectra. The increase in oxygen containing functional groups is seen as a direct effect of photo-oxidation of LDPE due to weathering which results in the generation of polar groups such as hydroxyl, ketone, carboxyl, aldehyde, ester etc. As expected, O/C ratio for humid weathering is high in comparison with dry weathering, due to the increased presence of OH groups on the LDPE.

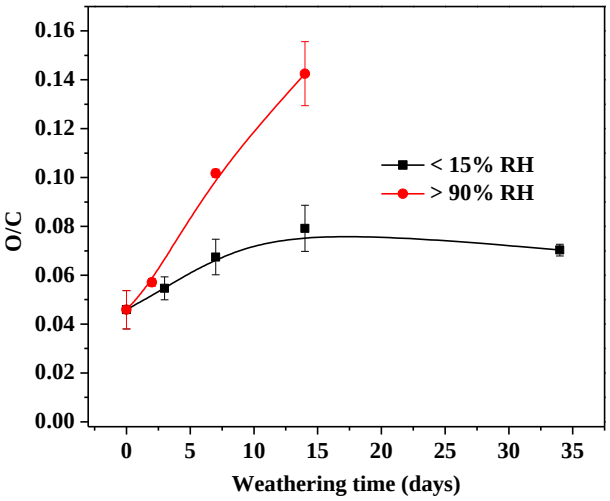

Figure 13: Dependence of O/C on weathering time in days for LDPE.

The O/C ratio gives only the rough estimate of the effect of the photo-oxidation. To determine the type of oxygen-carbon bonds of different functional groups, curve fitting of C1s peak has to be done. The deconvolution of C1s yields four peaks namely, C-C / C-H at 285 eV, C-O at 286.5 eV, C=O at 288 eV and O-C=O at 289.5 eV. Due to the influence of photo-oxidation these functional groups is seen as a kink or a shoulder to the c1s peak. A model deconvoluted C1s peak for UV weathered LDPE is shown in Figure 14.

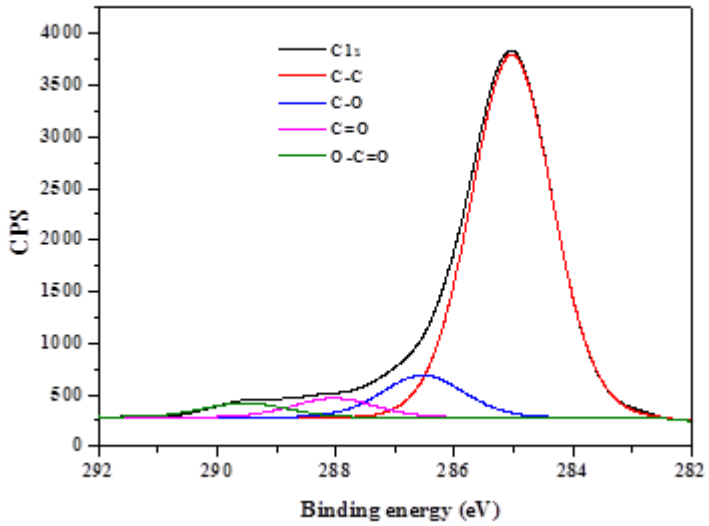

Figure 14: A model deconvolution of C1s peak of 6 days weathered LDPE

When a neat LDPE foil is weathered, the surface oxidation is seen as a decrease in the C1s peak at 285.0 eV which indicates the decreased concentration of un-oxidized carbon atoms. Figure 15 shows the C1s peaks of LDPE dry and humid weathered at 14 days, it can be seen that the effect of humidity is seen as increased intensity between 288 and 290 eV due to more oxygen containing functional groups. Whereas, in the case of <15% RH, the oxygen induction is still high.

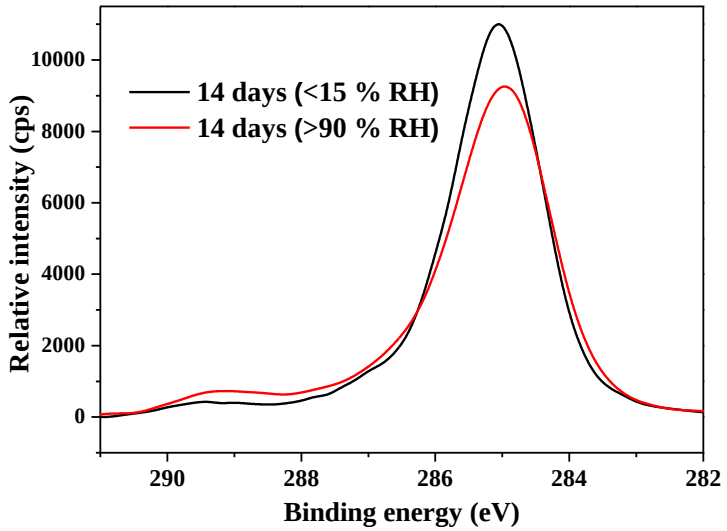

Figure 15: Comparison for C1s of 14 days LDPE weathered at <15% RH (black) and >90% RH (red).

When the weathering time increases the intensity of C-O bonds also increases which is possibly due to the more pronounced introduction of hydroxyl groups in the form of alcohols (C-OH) or hydroperoxides (C-O-OH), additionally ethers (-C-O-C-) may be introduced. Then the peak at 288 eV could be assigned to C=O bonds which is present in ketones [-C=O], or aldehydes [-CH=O]. The values are given in Appendix Table I-II.

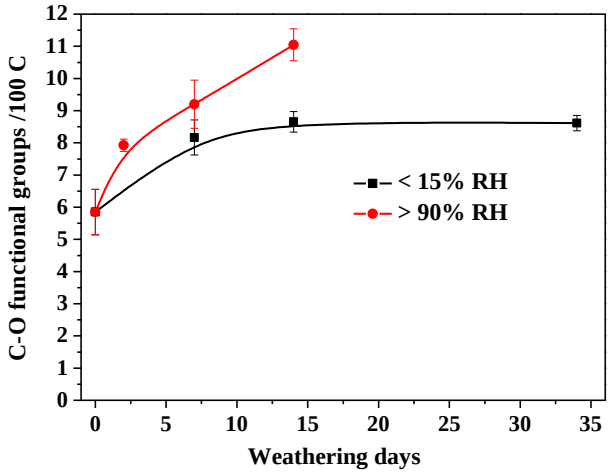

Figure 16: Dependence of C-O concentration on weathering period in days for dry (black) and humid (red) conditions.

Finally, the peak at 289.5 eV which correspond to the O=C-O bonds due to esters [-(CO)-OR-] and carboxylic acids [-(C=O)-OH or shortly COOH]. Carbon bound with three single bonds to oxygen may also appear at 289.5 eV. The intensity of these functional groups increases with prolonging weathering period and finally the foil could not be weathered beyond 32 days for <15% RH and for >90% RH the foils were too brittle by 14 days as shown in Figures 16-18 .

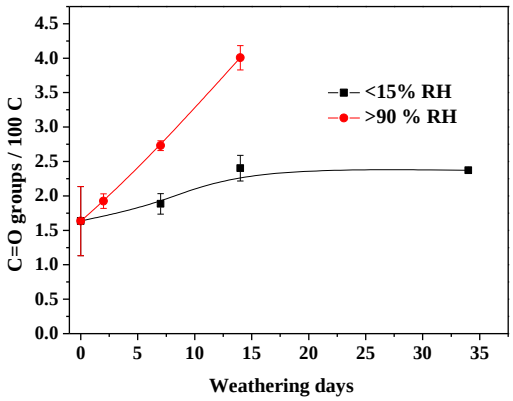

Figure 17: Comparison for C=O concentration for LDPE weathered at <15% RH (black) and >90% RH (red) against weathering period in days.

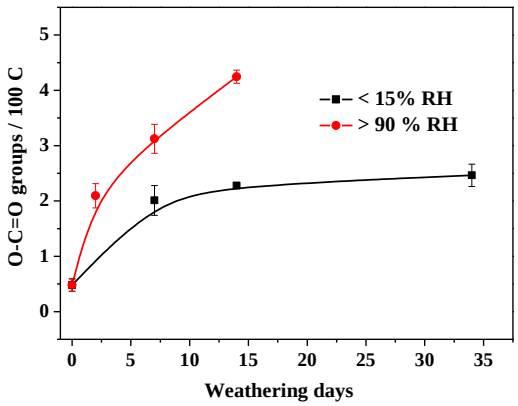

Figure 18: O-C=O concentration for LDPE weathered at <15% RH (black) and >90% RH (red) against weathering days.

Bulk analysis

DRS results

Figure 19 shows the dielectric loss ε'' as a function of temperature at a frequency of 1000 Hz. The dielectric loss is weak for the unirradiated sample (see 0 days) because of the absence of an intrinsic dipole moment as discussed above [56,99,100]. The weak dielectric losses for the unweathered sample could be due to the presence of some impurities, the effect of storage or the induction of oxygen during processing [101]. UV irradiation creates C-C chain scissions or H-abstraction, which generates polar radicals that act as a probe for molecular mobility in the samples by dielectric spectroscopy. The increase in dielectric loss with weathering is an indication of photo-oxidation which results in the generation of polar groups such as hydroxyl, ketone, carboxyl, aldehyde, ester etc. The peak around 50°C in the irradiated

samples is the α_c relaxation which is attributed to molecular fluctuations in the crystalline domains and appears as a shoulder to the β relaxation process near high temperature values. As discussed previously, the nature of these molecular fluctuations is still under discussion. Unlike mechanical relaxation, dielectric relaxation gives only one α_c peak whereas, mechanical spectroscopy reveals that the α relaxation is a more complex process and consists of two overlapping peaks (α and α'). There can be two reasons for α relaxation, first, the presence of different groups like ketones, esters etc. where the relaxation is due to the twisting of chain segments having carbonyl groups about their axes. Second, the net rigid motion is translation of the entire lattice along the c-axis. Latter is more prominent in mechanical relaxation of LDPE.

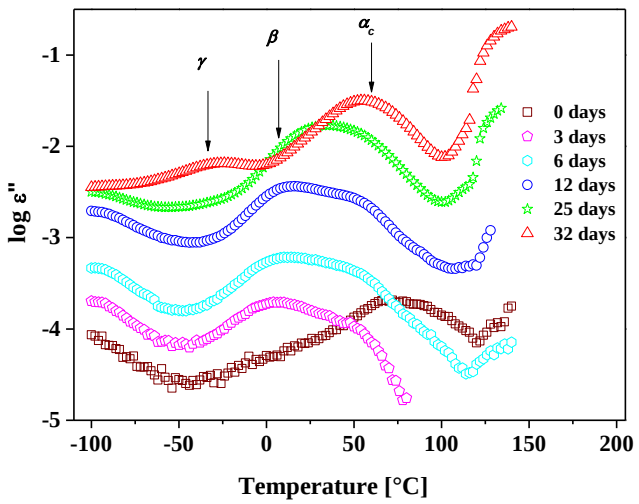

Figure 19: Dielectric loss ε'' vs. temperature at a frequency of 1000 Hz for 0 (square), 3 (pentagon), 6 (hexagon), 12 (circle), 25 (star) and 32 (triangle) days of weathering at <15% RH. The three relaxation processes namely α_c, β, γ appears in order of decreasing temperature (The γ relaxation is observed only for 25 (star) and 32 days (triangle) weathered LDPE) in the given temperature range.

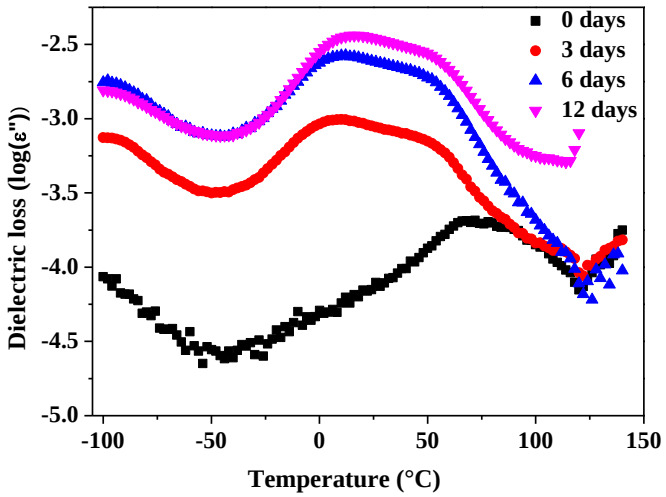

Figure 20: Dielectric loss ε'' vs. temperature at a frequency of 1000 Hz for 0 (black), 3 (red), 6 (blue) and 12 (cyan) days weathered LDPE at >90% RH.

Figures 19 and 20 show the dielectric losses as a function of temperature for LDPE weathered foils at <15% and >90% RH. In both the results, the broad peak occurring below 0°C is called β relaxation and is related to segmental fluctuations taking place in the amorphous domains of PE. It is responsible for the dynamic glass transition of polyethylene [102]. Besides the increase of the dielectric loss, the degree of photo-oxidation was also observed as a shift of the maxima of the β relaxation towards higher temperatures (see Figure 19) [49-53,99,100]. In Figure 19, it could be noted that the peaks of β relaxation and α_c relaxation become super imposed at higher stage of weathering [61].

The γ relaxation process is related to the localized fluctuations in the amorphous regions [103,104]. It is believed to that the UV irradiation has less impact on the γ process compared to α_c and β relaxation.

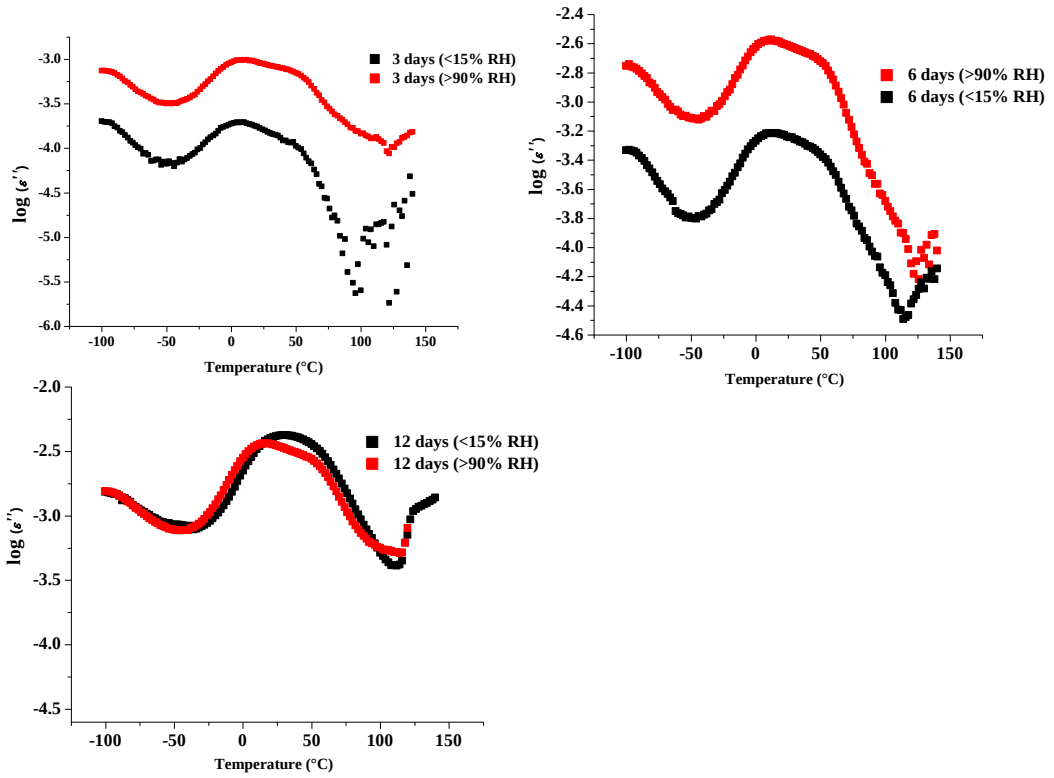

Figure 21: Comparison of dielectric losses at 1000 Hz for dry (black) and humid (red) weathered LDPE.

Figure 21 shows the comparison of dielectric losses of dry and humid weathered LDPE, the increased polarization is due to the effect of humidity for the LDPE weathered for 3 and 6 days at >90% RH . In the case of 12 days weathering period, the foils had reached the stage of disintegration due to prolonged weathering under high humidity. In the case of dry weathered sample the oxygen induction time was still high in the amorphous region and hence the β relaxation was seen shifting towards α_c relaxation till the point of destruction i.e. 32 days.

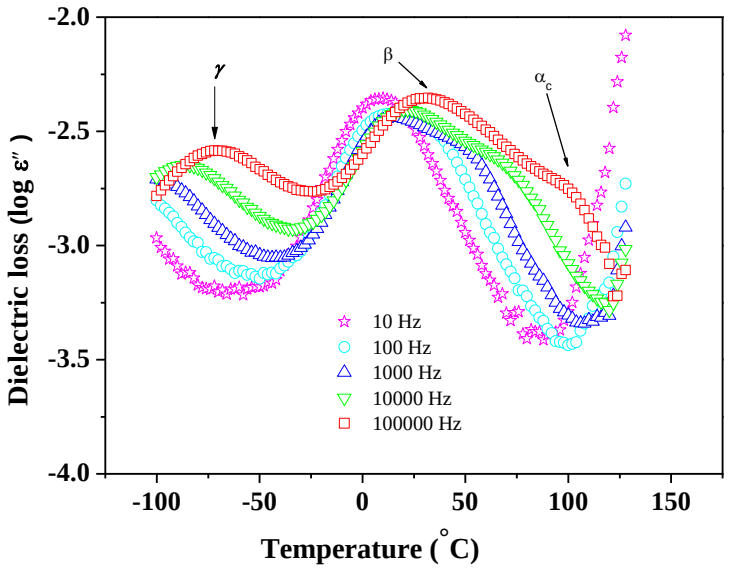

Figure 22: Dielectric loss vs. temperature after 25 days of weathering for different frequencies: 10 Hz (star), 100 Hz (diamond), 1000 Hz (triangle), 10000 Hz (Inverted triangle) and 100000 Hz (square).

Figure 22 shows the dielectric loss vs. temperature at different frequencies for 25 days of weathering. The γ relaxation process shifts in the experimental accessible temperature range for higher frequency [105]. As expected all relaxation processes shift to higher temperatures as the frequency is increased.

Usually the model function of Havriliak-Negami (HN) is used to analyze relaxation processes quantitatively [106,107,108].

$$\varepsilon^*_{HN}(f, T = const.) = \varepsilon_\infty + \frac{\Delta\varepsilon}{[1 + (i\frac{f}{f_{HN}})^\beta]^\gamma}$$

Since PE has a very weak dielectric response, it was difficult to fit the HN function to the relaxation spectra in the frequency domain. So the spectra were plotted in the temperature domain, i.e. the dielectric loss is plotted versus temperature for different frequencies. For each frequency, the temperature relating to the maxima of dielectric loss was estimated from these plots for the different relaxation processes and was plotted in the relaxation map.

For example, the relaxation map for 25 days of weathering is shown in Figure 23. For all relaxation processes the temperature dependence of the relaxation rates can be approximated by the Arrhenius equation:

$$f_{\max} = f_{\infty} \exp\left(-\frac{E_A}{RT}\right)$$

where R is the gas constant, f_{∞} is the pre-exponential factor and E_A is the activation energy. It is known that for the β relaxation related to glassy dynamics, the temperature dependence of f_{max} should be curved when plotted versus 1/T which can be well described by the Vogel/Fulcher/Tammann formula [109-111]. This is not observed here and the reason for this discrepancy is not clear and needs further investigations. Nevertheless, the estimated prefactors are in the order of 10^{16} which indicates that the β relaxation is not a simple activated process.

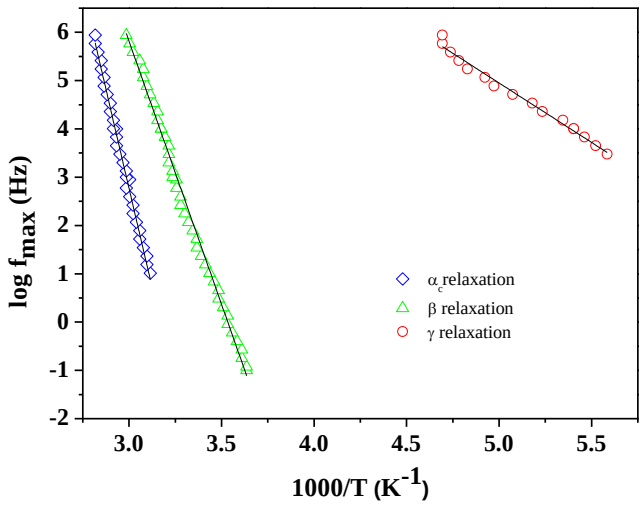

Figure 23: f_{max} for the three relaxation processes: α_c (diamond), β (triangle) and γ (circle) for 25 days weathered LDPE at 1000 Hz. The solid line is a linear fit to the corresponding data for each relaxation process.

The discussion of the influence of UV weathering on different relaxation processes in LDPE is organized in the following way. The β relaxation is the most prominent process in dielectric loss (see Figures 19-20). The α_c relaxation is also affected by UV weathering whereas the γ

relaxation is only weakly influenced by the weathering. Therefore, this process is not discussed further.

β relaxation process

Figure 24 shows the relaxation map for the β relaxation process for different weathering periods at dry condition. Because of the fact that the β relaxation is due to segmental fluctuations in the amorphous domains, the changes in the dielectric loss must be related to the amorphous regions. Increase in weathering time leads to a systematic shift in β relaxation to higher temperatures.

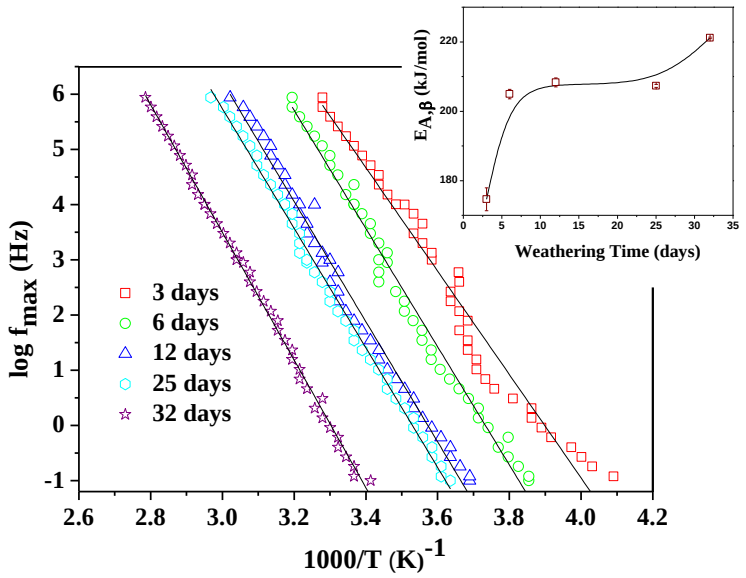

Figure 24: Relaxation rates f_{max} vs 1/T for the β relaxation process for different weathering times, 3 days (square), 6 days (circle), 12 days (triangle), 25 days (hexagon), and 32 days (star). The solid lines are fits of the Arrhenius equation to the corresponding data. The inset shows E_a as a function of the weathering time for the β relaxation.

When LDPE is weathered, chain scission and generation of radicals take place as discussed before. The formed radicals can undergo crosslinking reactions. In addition, the effect of chain scissions leads to decrease in the molecular weight. Shorter chains can crystallizes more easily than longer ones. Another possibility is the formation of hydrogen bonds between oxygen containing functional groups and thus, hydrogen bonds and physical interactions of polar groups can also enhance the chemi-crystallization [112,113].The plateau region between 12 and 25 days of weathering can be understood by the following considerations. Chain

scissions lead the chain ends to dangle which in turn creates free volume. In general, an increase in free volume will decrease the glass transition temperature. So, the plateau in the weathering time dependence can be assigned to a counter balance between an increase of the glass transition temperature due to crosslinking and/or crystallization and a decrease of it due to the creation of free volume. The activation energy of the β relaxation was determined by fitting the Arrhenius law to the corresponding data and plotted versus the weathering time (see inset Figure 24). Relatively high values of the activation energy and prefactors are found which indicates that the β relaxation is a cooperative process.

In the case of weathering with higher humidity > 90% RH, since LDPE in question is a semi-crystalline polymer, the probability of permeation of water is possible only in the amorphous regions than in the crystalline region, due to the tightly packed structure [114]. Careful observation of dielectric loss graph (Figure 20) also shows a slight shift of β relaxation maxima towards higher temperature implying the segmental motions in amorphous domain.

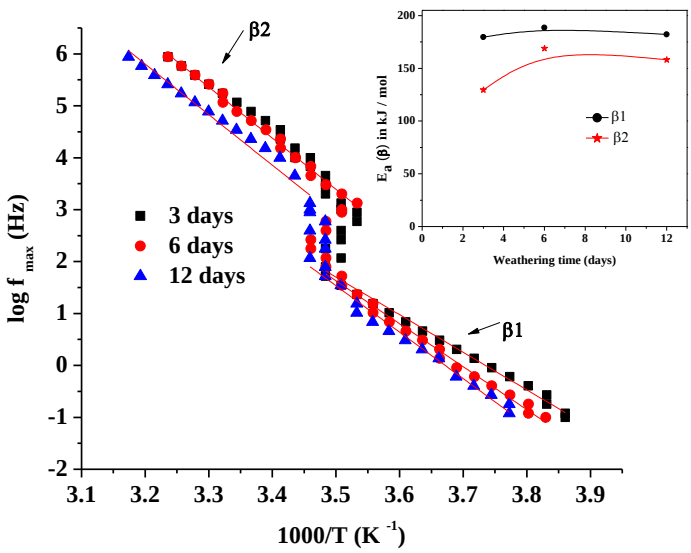

Figure 25: Relaxation rates f_{max} vs. 1/T for the β relaxation process for different weathering times, 3 days (black), 6 days (red) and 12 days (blue) weathered at >90% RH. The solid lines are fits of the Arrhenius equation to the corresponding data. The inset shows the activation energy (E_a) as a function of the weathering time for the β relaxation.

The relaxation map of β relaxation is shown in Figure 25 for all frequencies. Since water has a dipolar character and it is dielectric active. The reason for the kink near 283 K for all weathering days is still not clear and needs further research. It was assumed that could be an indication of water permeation and while heating the sample during measurement the traces of water can defreeze after 0°C. According to literatures, the water molecules were assumed to act as a plasticizer in the LDPE and able to form hydrogen bonds with the polymer chain [115,116]. But still, the plasticization effect and the nature of interaction of water molecules with polymer chains in the amorphous regions are widely debated and it is still under discussion. Another way of analysing the relaxation map is the activation energy plot which is calculated from the Arrhenius equation. In β relaxation, there are two kinds of behaviour β_1 and β_2 corresponding to the frequency ranges 100 Hz and 10 kHz respectively. The activation energies for 3 and 6 days weathered LDPE at higher humidity is lesser than the one weathered at <15% RH. It can be due to the interaction of water molecules with the polymer chains thereby making the chains less mobile. Another reason could be these water molecules fill up most of the free volume and form van der Waals bonds with the carbonyl groups (C=O) or at the terminal –OH groups. The induced water molecules in the amorphous regions must contribute to the existing molecular polarization, which has higher probability to occur at the terminal –OH groups, since these also has significant dipole moment and also seems to be behind the decrease of dielectric constant for β relaxation. This implies that water molecules become immobilized due to the reduction in the free volume in the semi-crystalline region and also due to presence of carbonyl groups [115-116].

α_c relaxation process

Figure 26 shows the relaxation map for the α_c relaxation processes in dependence of the weathering time under dry condition. Similar to β process the temperature dependence of the relaxation rates can be described by an Arrhenius equation for all weathering times. The activation energies for 3, 6, 12, 25 and 32 days are as follows: 108.5, 123.5, 130.9, 314.7 and 219.5 kJ/mol respectively, (see inset of Figure 26). It can be interpreted as follows, the motional processes in crystallites are responsible for the α_c relaxation process and it is seen

that there are no significant changes in the activation energies of α_c loss peaks for 3, 6 and 12 days of weathering. During the initial stages of weathering the dipole fluctuations in the crystallites do not change which is in agreement with the DSC result. The degree of crystallization changes strongly for weathering periods longer than 12 days. In agreement with the line of argumentation presented above the behaviour for shorter weathering times could be interpreted as the induction period for chain-scission and/or crosslinking in the amorphous regions. An increase in the activation energy of the α_c process was observed for 25 and 32 days of weathering implying that the structure of the crystalline phase is changed due to the re-arrangement of the shorter chains in the amorphous regions. This means both an increase of the degree of crystallization and a perfection of existing crystals, where especially the latter point is responsible for the strong increase of the activation energy. This is also supported by the shift of β relaxation peaks towards the α_c process as shown in Figure 19.

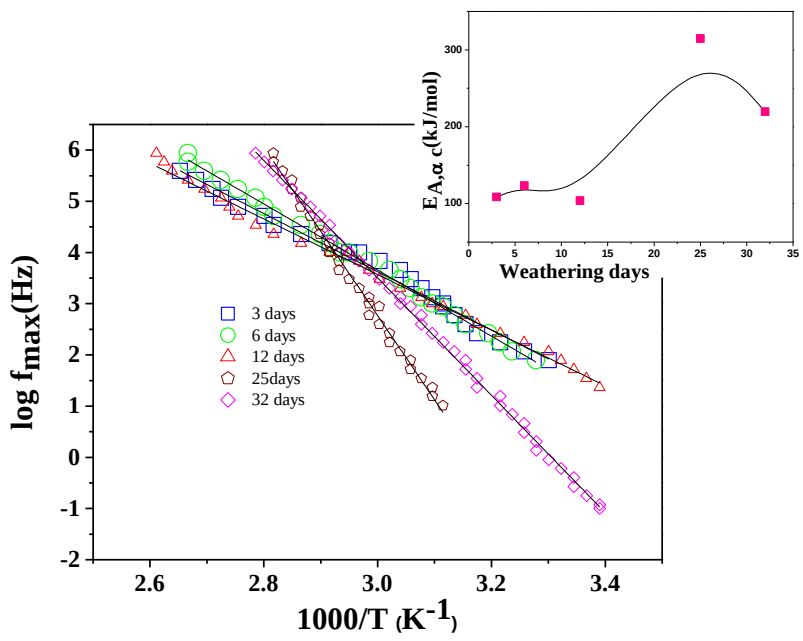

Figure 26: Relaxation rates f_{max} vs. 1/T for α_c relaxation processes for 3 days (square), 6 days (circle), 12 days (triangle), 25 days (pentagon) and 32 days (diamond). The solid lines are linear fits of the Arrhenius equation and slope gives the activation energy. The inset shows the activation energy (E_a) as a function of weathering time for α_c relaxation.

The inset of Figure 26 shows the temperature dependence and the inset shows the activation energies of the α_c relaxation process as a function of weathering period. The crystallinity increases sharply after 12 days and finds its maxima for 25 days of weathering. The activation energy slightly decreases after 25 days of photo-oxidation and drops for 32 days weathered LDPE due to much less available space for further arrangement of the short chain segments and causing embrittlement.

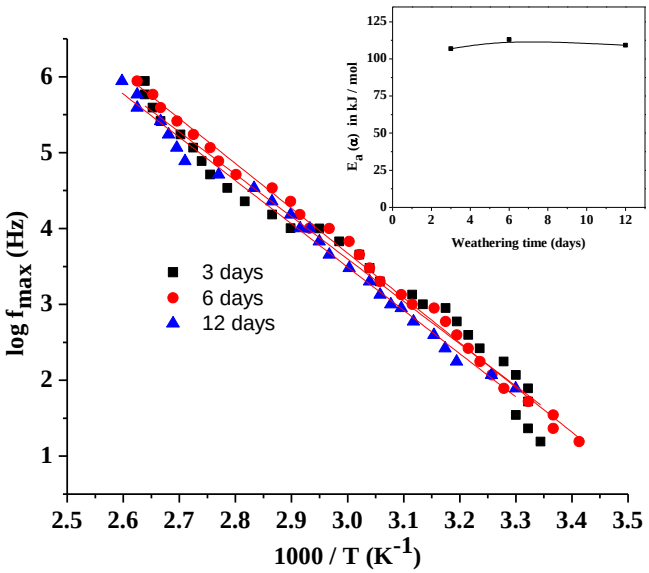

Figure 27: Relaxation rates f_{max} vs. 1/T for α_c relaxation processes for 3 days (black), 6 days (red), 12 days (blue) weathered at >90% RH. The solid lines are linear fits of the Arrhenius equation and slope gives the activation energy. The inset shows the activation energy (E_a) as a function of weathering time for α_c relaxation.

Figure 27 shows the relaxation rates α_c relaxation for LDPE weathered under higher humidity. The activation energies (see inset) for α_c relaxation for 3 and 6 days are almost same as neat LDPE (110 kJ/mol). This could be an indication that humidity or interaction of water molecule with the polymer chains does not affect the α_c relaxation peaks or no significant impact in the crystalline domains.

Dielectric strength

The Debye theory of dielectric relaxation generalized by Kirkwood and Fröhlich gives for the dielectric strength [57]:

$$\Delta\varepsilon = \frac{1}{3\varepsilon_0} g \frac{\mu^2}{k_B T} \frac{N}{V}$$

Where μ is the mean dipole moment related to the process under consideration and *N/V* is the number density of the dipoles (in this case: radicals generated due to weathering). *g* is the Kirkwood/Fröhlich correlation factor which describes the static correlation between the dipoles. k_B is the Boltzmann's constant. The Onsager factor describing internal field effects is omitted for the sake of simplicity. ε_0 is the permittivity of free space.

The dielectric strengths of α_c is due to fluctuations of polar groups within the crystallites and the dielectric strengths of β relaxation refers the number density of dipoles in the amorphous regions.

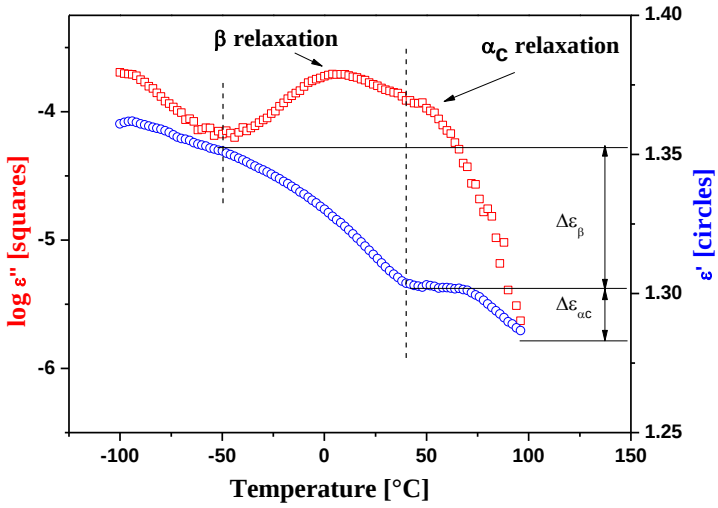

Figure 28: ε' (circles) and ε'' (squares) vs. temperature for three days weathered LDPE at f = 1 kHz indicating the dielectric strengths of β and α_c relaxation. The absolute values of ε´are subjected to errors because no gold electrodes are deposited at the samples.

Normally the dielectric strength is estimated by fitting a model function to the data which is not possible here. Therefore dielectric strengths are estimated as shown in Figure 28. Figures 29 and 30 show the change of dielectric strengths of α_c and β processes as a function of weathering days for both dry and humid conditions. In Figure 29, $\Delta\varepsilon_\beta$ increases with increasing weathering up to 6 days (see inset) which is due to an increasing number of dipoles. The decrease in $\Delta\varepsilon_\beta$ after 6 days could be attributed to crosslinking because $\Delta\varepsilon_{\alpha c}$ remains approximately constant up to a weathering time of 12 days. $\Delta\varepsilon_\beta$ increases further after 12 days, such increase, points to a further formation of radicals and consequently, destruction of the network.

The dielectric strengths of the α_c process did not depend on the initial weathering periods. Because $\Delta\varepsilon_{\alpha c}$ is due to the number of dipoles fluctuating in the crystallites this means that the structure of the crystallites is not changed which is in agreement with the DSC results. After this induction period the dielectric strength increases with increasing weathering time implying increase in crystallinity again in agreement with the DSC results.

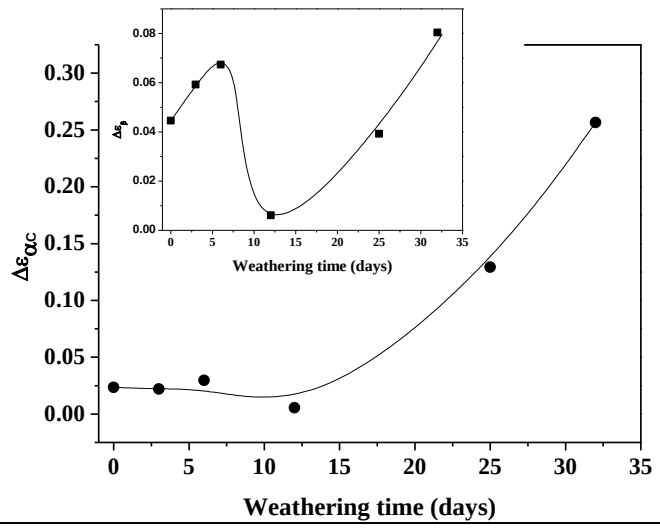

Figure 29: Dielectric strengths of the α_c relaxation vs. weathering period. The inset gives $\Delta\varepsilon_\beta$ vs. the weathering time.

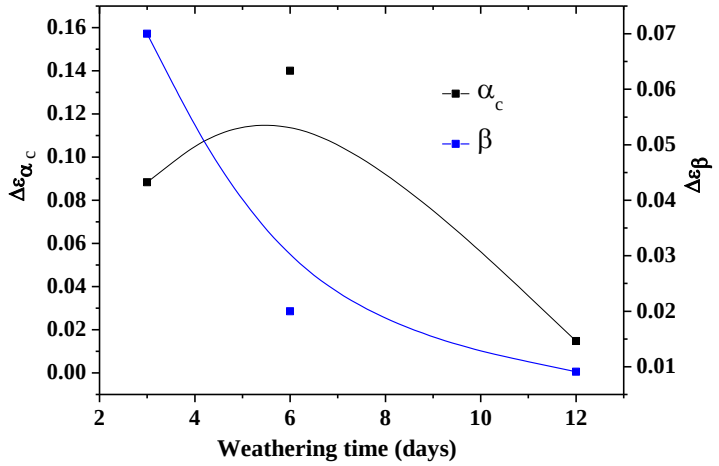

Figure 30: The dielectric strengths for α_c and β relaxation modes for LDPE weathered at 60°C with >90% RH

In Figure 30, the decrease in the dielectric strength for α_c and β relaxation modes could be a combined effect of cross linking and reaction of radicals with the OH groups which hinders the mobility of polymer segments.

DSC

Crystallization behaviour of the weathered PE samples was investigated by DSC. The change of enthalpy for melting are plotted as a function of exposure time for samples weathered in dry condition is shown in Figure 31. In principle, it would be recommended to compare the glass transition measured by DSC. Unfortunately no glass transition phenomena can be detected by DSC for semi-crystalline LDPE as discussed in [117]. The enthalpy values can be taken as an estimate for the degree of crystallization. The results obtained by the first heating should also be discussed in detail here because of the fact that information of weathering of the pristine samples will be obtained. For the second heating the samples are melted and recrystallized which leads to a changed behaviour. For shorter weathering times the enthalpy decreases but increases strongly for weathering periods longer than 6 days. This increase is observed in both the first and the second heating run. The decreasing of the degree of crystallization during shorter weathering periods can be explained by an induction time dominated by chain scission and/or crosslinking. Therefore the initial increase of the glass

transition temperature can be attributed to crosslinking or the formation of hydrogen bonds. For longer weathering times the degree of crystallization increases which also leads to an increasing brittleness in the weathered polymer. For foils weathered at >90% RH, DSC showed no remarkable change in the melting point of LDPE.

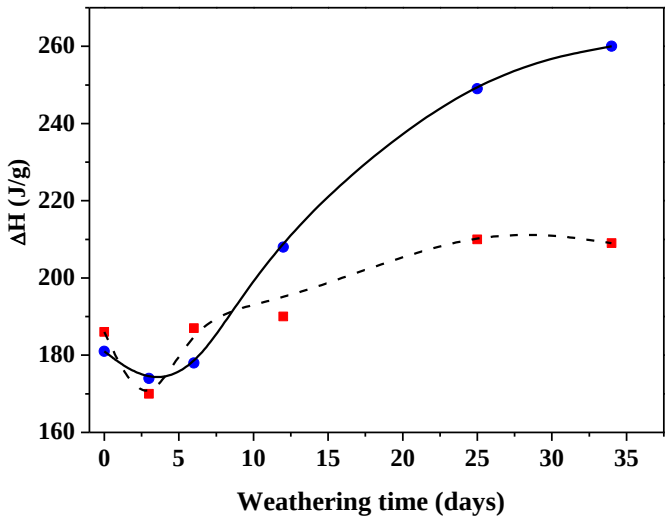

Figure 31: Change of enthalpy of melting (ΔH) as a function of weathering period at <15% RH: circles-first heating; squares –second heating.

Micro-tensile measurements:

The mechanical properties like Young's modulus and elongation at break (%) for artificial weathered LDPE films at <15% and >90% RH were studied using micro-tensile measurements as mentioned in Chapter 3.4. In the weathered sample of 3 days alone, the films were brittle and while clamping on both the ends, the films were broken. So, mechanical testing could not be carried out for higher weathering days. From the unweathered foil, it was found that neat LDPE foil was too ductile as shown in Figure 35 (0h curve) under Chapter 4.2.

4.2. Oxygen plasma weathering of LDPE at 50 W

LDPE films were exposed to radio frequency (RF) low pressure oxygen plasma over a longer time to see is there any change in the surface and/or bulk properties. The working power was set to 50 W, as higher power values for longer exposure might over heat the sample surface and can damage the foils. Samples were treated under O_2 low pressure plasma with experimental conditions explained in Chapter 3.4.

Surface effects

XPS

As discussed before in the Chapter 4.1, the XPS spectrum of a neat low density polyethylene shows only the C-C or C-H symmetric peak centered at 285.0 eV. Figure 32 shows the O/C ratio as a function of plasma treatment time and the high amounts of O/C is due to the vacuum UV radiation and other energetic species in the plasma. After 30 min plasma treatment, O/C ratio reaches a plateau and after 240 min of treatment only 14% oxygen groups have been formed. Which is equivalent to the XPS results of 25 days of artificial weathering under <15% RH.

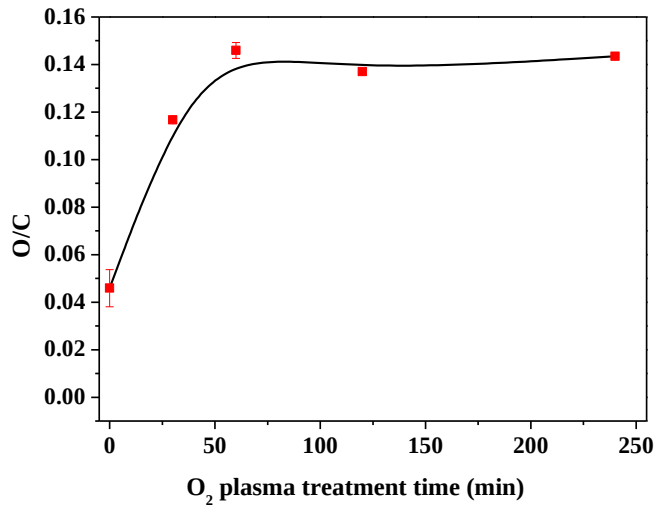

Figure 32: O/C vs. Oxygen plasma treatment time in min for LDPE.

The generated C-radical sites could react with oxygen when the LDPE was exposed to ambient air, post-oxidation occurs and forming peroxy radicals and hydroperoxides. The

scheme of these reactions leading to a variety of oxidation products was suggested by many literatures [118-123].

$$C^{\bullet} + O^{\bullet} - O^{\bullet} \rightarrow C - O - O^{\bullet}$$

$$C - O - O^{\bullet} + RH \rightarrow C - O - OH + R^{\bullet}$$

Most oxygen functionalities like C–O (alcohol), C=O (carbonyl), COO (carboxylic acid, ester), etc. are formed from the hydroperoxides. Figure 33 shows the results of deconvolution of C1s peak: C–O (hydroxyl, ether) at 286.5 eV, that of C=O (carbonyl or aldehyde or O-C-O structures double ether) at 288 eV and finally O-C=O (ester or carboxylic acid) to 289.5 eV. Similar to artificial weathering, there was no big change in the amounts of C=O and COO groups. These oxygen containing functional groups have one thing in common: till 30 min of oxygen plasma treatment the increase is steep and considered to be the induction time for chain-scission and generation of radicals. After that till 240 min there is not much significant changes in the concentration, this region is termed as the steady state. The values are tabled in A.T. III.

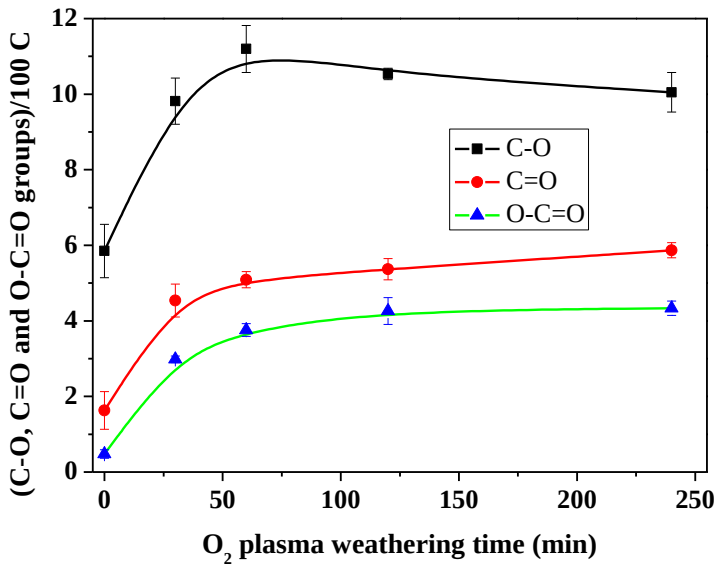

Figure 33: Oxygen functional groups per 100 C vs. Oxygen plasma treatment time in min for LDPE

In contrast to the XPS results, ATR-FTIR showed no significant change on the surface properties of LDPE for oxygen plasma treatment longer than 200 min. It was assumed that the effect of photo-oxidation induced by oxygen plasma is limited to the few tenths in nm. Since the sampling depth of ATR-FTIR is 2.5 µm, the effect is not as pronounced as in the case of XPS as shown in Figure 34. Another reason could be the low power value of 50 W, few researchers have tried around 300 W and have seen some changes in the FTIR spectra with pronounced C=O stretching at 1700 cm^{-1}. The effect of oxygen plasma exposure is limited to the topmost surface due to the formation of radiation-shielding groups at the surface such as polyenes or carbonyls [120].

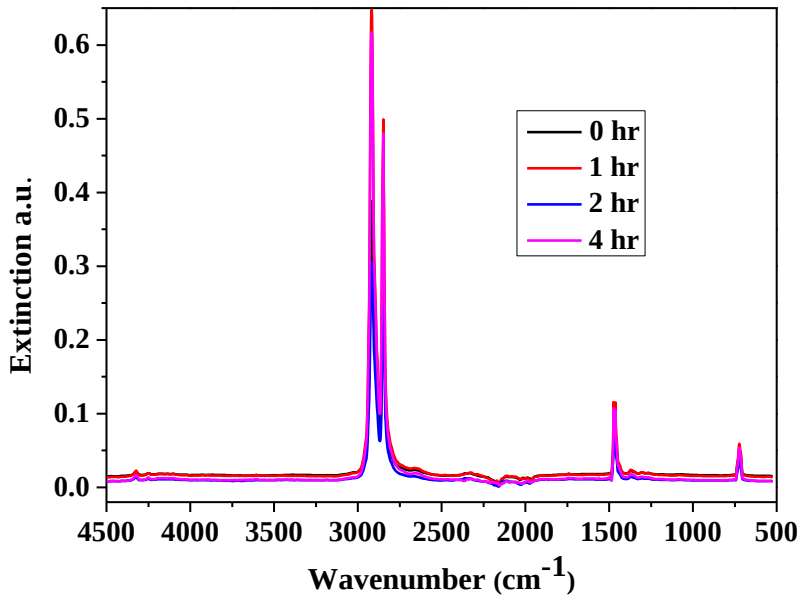

Figure 34: ATR-FTIR spectra for LDPE treated with oxygen plasma for different time in hour.

Micro-tensile measurements for O_2 plasma treated LDPE:

The experimental settings for micro tensile strength are same as mentioned in Chapter 3.4. The force as a function of displacement for LDPE is shown in Figure 35. Ductility was common in all oxygen plasma treated LDPE foils.

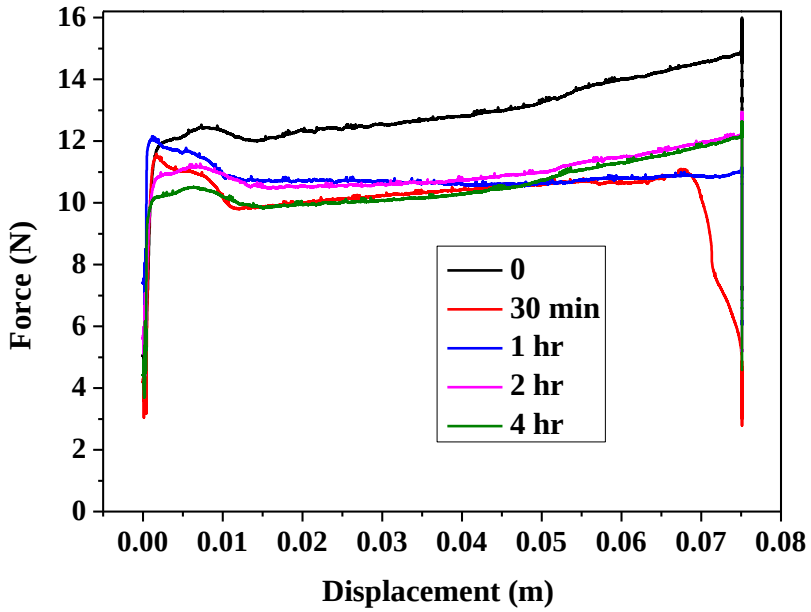

Figure 35: Force (N) vs. displacement (m) for oxygen plasma treated LDPE at different time in hour.

It was found that the oxygen plasma has a little effect on the 4h treated film compared to neat LDPE. The yield strength shows a reduction when compared for 4h treated LDPE with neat sample. The force taken by the 4h treated sample in the necking region is less when compared to the necking region of the neat LDPE. In all the treatments, the ductility is found to be common as seen in Figure 36. The elongation at break also did not show any evidence for change in the bulk properties for 4h treatment. The errors concerned with the measurements were around ±10%.

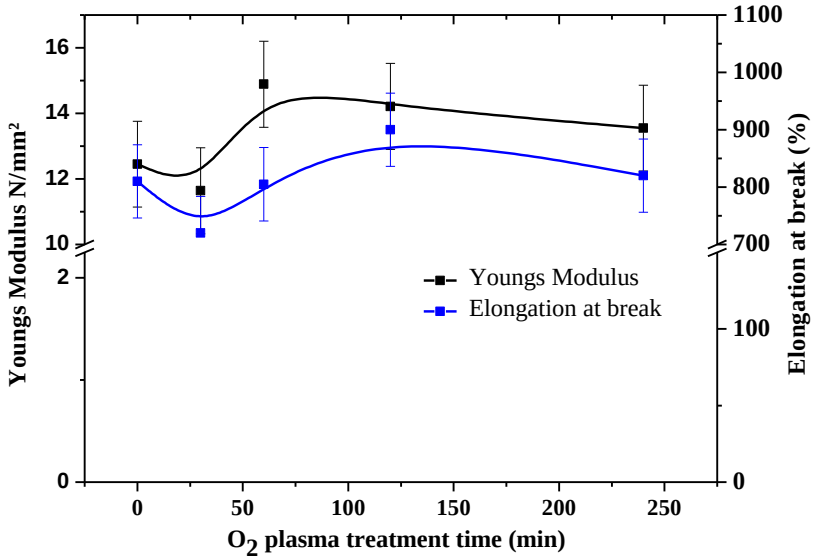

Figure 36: Young's modulus (black) and Elongation at break (blue) in % for oxygen plasma treated LDPE at different time in hour.

LDPE did not show much acceleration effect because of less penetrative effect into the bulk by plasma. In addition, the different species present in the plasma induce the formation of free radicals in the polymeric chains and in this way it is possible to insert or interlock certain functional groups on the polymeric surface; this will have a positive effect on the functionalization/activation of the polymer surface [124]. The surface or bulk analysis was done immediately after the oxygen plasma treatment, hence there could be only surface effects and the bulk properties show no significant changes. The post plasma ageing might have an effect on the bulk [120].

Nature of LDPE surface photo-oxidation after Ar plasma followed by Br gas

It is understood that by introducing bromine without plasma assistance (gas phase) the radical oxidation can be slowed down or eliminated. Bromine can act as a radical scavenger at the surface and in near-surface layers of polyolefins:

$$Polymer\bullet + Br_2 \rightarrow Polymer\text{-}Br + \bullet Br$$

$$Polymer\bullet + \bullet Br \rightarrow Polymer\text{-}Br$$

Besides the reaction between C-radical sites and molecular bromine shown above, the electrophilic addition of bromine across the C=C double bonds in alkenes have to be also considered [83]:

$$> C = C < + Br_2 \rightarrow > CBr - CBr <$$

XPS was used to quantify the introduced bromine concentration on the polymer surface within its sampling depths of maximal 6 nm. The presence of bromine was confirmed by the Br $3d_{3/2+5/2}$ (70.2 eV), Br $3p_{3/2}$ (183.1 eV) and Br $3p_{1/2}$ (189.72 eV) peaks in the XPS spectra [125]. Therefore, the post-plasma bromination method can be applied for raw quantification of radicals or C=C double bonds that are formed on polyolefin surfaces due to plasma irradiation [126].

Argon plasma treatment of polyolefins

The untreated PE foils were checked by XPS for any impurities on the surface, however, which could not be detected. Smaller concentrations of oxygen (O/C of 0.013 for PE) could be attributed to additives of polymer processing or due to storage.

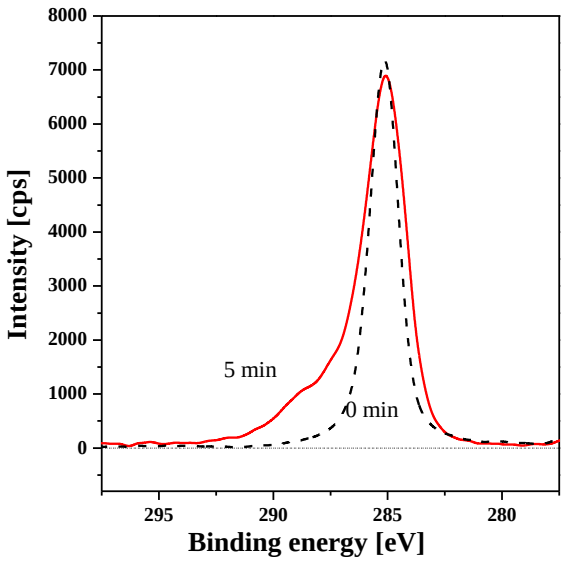

Figure 37:C1s peak broadening of LDPE after 5 min exposure to Ar plasma and 1 day to ambient air

LDPEs were exposed to argon plasma for 0.5, 1, 2 and 5 min at 100 W and 10 Pa. Due to the inert nature of argon, in principle, argon plasma does not introduce any new

functional groups in the polymer unlike other plasmas such as oxygen, nitrogen, ammonia etc. Nevertheless, argon plasma can sputter and therefore etch the surface by the plasma particle shower and the high-energy vacuum-UV irradiation may produce chain scissions, formation of radicals, double bonds and cross-linking, which results in broadened C1s peak [127]. Such broadening of C1s peak is presented for each 5 min exposure of polyethylene and polypropylene to Ar plasma and 1 day exposure to ambient air (Figure 37).

The resolved C1s peak shows the presence of O-containing polar groups characteristic for C-O (C-OH, C-O-C, C-O-OH, epoxy) at 286.8 eV, for >C=O, CHO, O-C-O at 287.5 eV and for O=C-OH(R) at 289.2 eV referenced to C-C or C-H bonded carbons of the polyolefin backbone at 285 eV [81]. However, more oxygen functional groups are tentatively present, such as carbonate (O-CO-O) and also hydroperoxy (-O-OH) or peroxy (-O-O-) [128]. The oxidation of C-radical sites is a rapid reaction of free radicals and a slow reaction of trapped radicals, which are situated in surface-near layers or even in the bulk of the sample. The peroxy radicals react with adjacent polymer chains forming hydroperoxides, which decay or rearrange to a broad variety of oxidation products [129]. The O/C ratios were plotted in dependence on time of exposure to the argon plasma as shown in Figure 38.

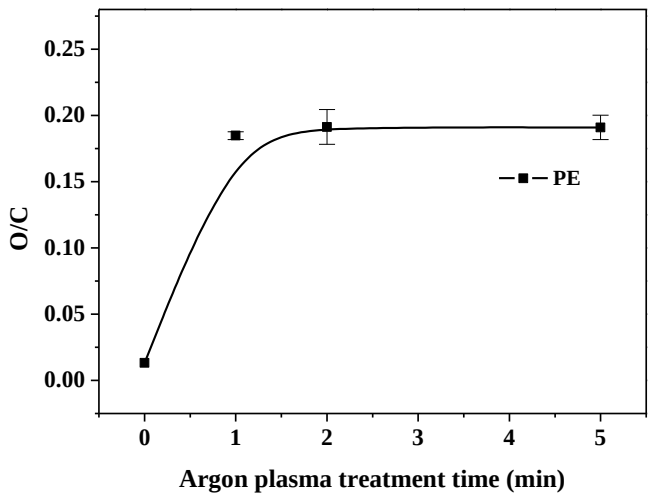

Figure 38. Variation of oxygen concentration on PE films after argon plasma for different times.

The O/C ratios for PE increase with exposure time and then level off after 1 min exposure at 0.19 and 0.24 respectively. The measured concentrations of oxygen confirm the presence of considerable concentration of C-radical sites in Ar plasma exposed polyolefins as also found in literature [97-98,130]. Argon plasma produced radicals on the surface can also react with one another from adjacent chains thus forming cross linked layers as found by Hansen and Schonhorn [131] and interpreted by Hudis [132].

Bromine gassing after Ar plasma exposure

Since polyolefins are non-polar and chemically inert, reactions at the surface can only be achieved by scissions of C-C and C-H bonds. C-C scission of backbone is undesired in contrast to C-H scission, which can be used for introducing functional groups. Exposure of polyolefins to Ar plasma and its radiation leads to scissions of C-C and C-H bonds, thus radicals and heat is produced (by immediate recombination) [135]. Besides free radicals a majority of radicals are metastable trapped in the bulk or near surface produced by irradiation with vacuum UV from plasma [133]. The action of metastable Ar atoms as proposed more recently is limited to a few Angstroms at the surface [127]. The trapped radicals in deeper layers are not able to recombine or to migrate along chains as they are shielded by adjacent chains or radical stabilizing bonds. Only molecular oxygen can diffuse into these layers to the trapped radicals, can react with them by auto-oxidation over longer periods of weeks, months or years [83]. Such long-living trapped radicals or stabilized free radicals can be labelled by radical scavengers as discussed before [78-80]. According to Elman et al. the rate constant for bromination is 1.4×10^{-7} s^{-1} which is slower than chlorination [82]. This is due to the thermodynamics of the chemical bromination. Basing on standard dissociation energies the bromination reaction enthalpy is endothermal and shows $\Delta_R H^{\Theta}_{298}$= 33 kJ/mole in comparison to chlorination ($\Delta_R H^{\Theta}_{298}$= -17 kJ/mole) [4].

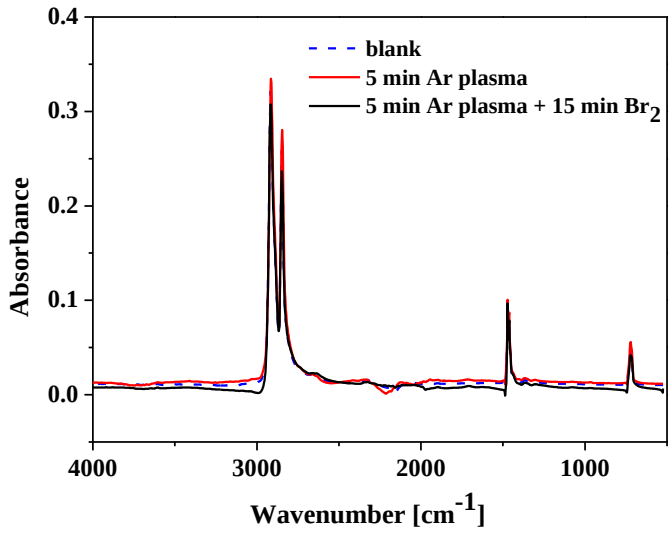

Figure 39: FTIR spectra of untreated (dash), argon plasma exposed (red) and then bromine gas treated LDPE (black)

Therefore, bromine can only react with radicals or activated C-H bonds and is therefore more or less suited for radical labelling. The situation may be more complicated because the size of bromine is slightly larger by 15% than that of oxygen, so surface uptake may be higher than the near-surface layers [80,134,135]. Another side-chain reaction of argon plasma is the dehydrogenation to olefinic double bonds or formation of conjugated double bonds [127,130]. Trans-vinylene (965 cm^{-1}), vinyl (910 cm^{-1}) and vinylidene (888 cm^{-1}) double bonds were found in the FTIR-ATR spectra before and after bromination according to (Figures 39 & 40) [136,137].

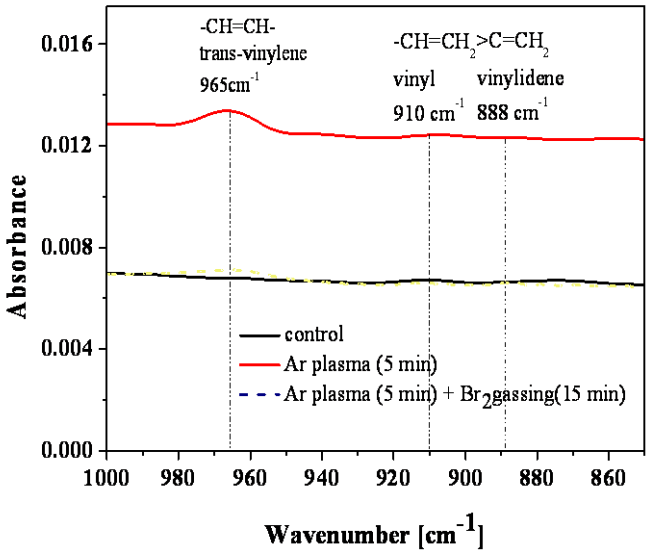

Figure 40: The vinyl, vinylidene and trans-vinylene groups of PE after argon plasma (red) which are quenched by Br gas after argon plasma (dashed) and untreated (black).

Ar plasma exposure had preferably produced mid-chain unsaturations rather often than new unsaturated end groups. Most of these double bonds were reacted by bromine as can be followed by the decrease in intensity of the band at 965 cm^{-1}.

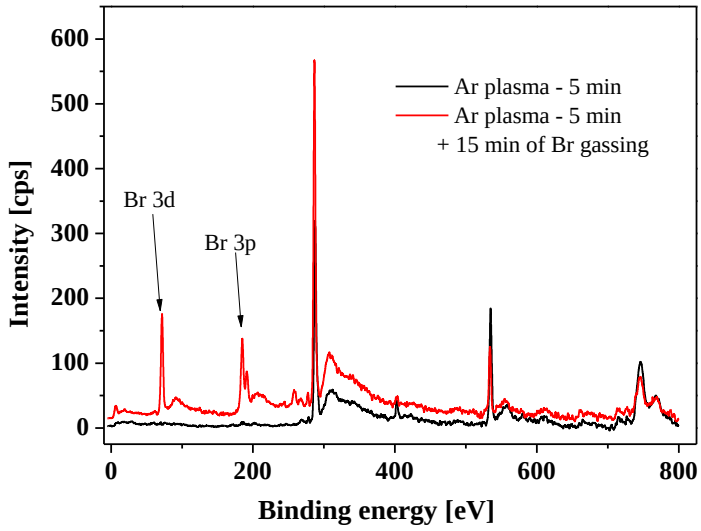

Figure 41: Comparison of XPS spectra of PE films, black line shows argon plasma treated for 5 min and red line represents 5 min of argon plasma followed by 15 min of bromine gassing.

Figure 41 shows the comparison of XPS spectra of argon plasma treated PE and argon plasma followed by Br gassed PE. The presence of Br $3d_{3/2+5/2}$ and Br $3p_{1/2}$, $3p_{3/2}$ peaks was found for Br gassed samples by Br peaks at binding energies at 70.2, 183.1 and 189.7 eV, respectively. These values agree well with the literature [134,135]. During argon plasma treatment (may be also a post-plasma effect) a few tracer gases like nitrogen were also present as impurity on the plasma chamber in very small concentrations as it is seen in the XPS spectra around 400 eV. Since the focus is on effect of post plasma bromination, the influence of nitrogen is omitted for the sake of simplicity. Figure 42 shows the ratios of O/C and Br/C against argon plasma treatment time for PE foils.

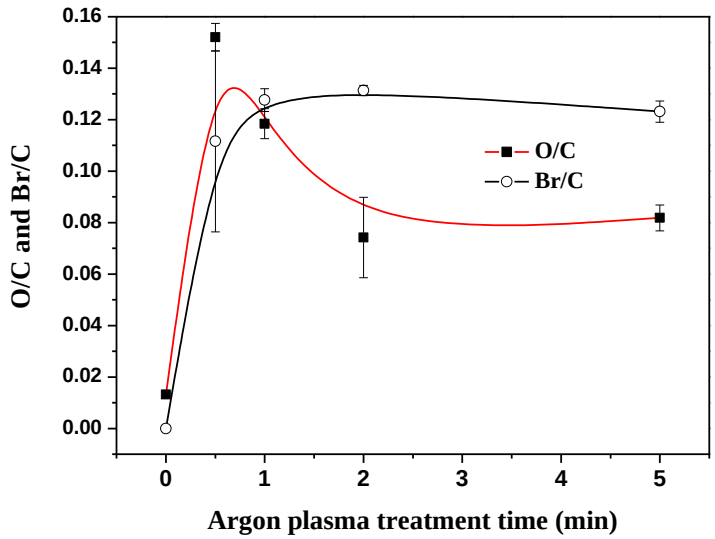

Figure 42: O/C (red) and Br/C (black) ratios for PE films treated with argon plasma for different times and exposed to bromine gas for 15 min after each treatment.

The increasing Br/C ratio with increasing plasma treatment time indicates the presence of bromine moieties on polyolefin surfaces and in near-surface layers (corresponding to the 6 nm sampling depth of XPS). In the case of PP, higher concentration of bromine has been found when compared to PE, can be attributed to the higher probability of H-abstraction from the tertiary C-atom than the secondary C-atom due to the stabilization of free radical by inductive effect of methyl groups or by hyper conjugation [84]. Primary, secondary and tertiary C-H bonds show reactivities towards bromine as 1:32:1600 [138]. Balamurugan et al.

found that the length of conjugation in brominated PP is much higher than that of PE due to decrease of C-Br bond energy in the order of 1°>2°>3°, which increases the rate of dehydro-bromination in PP [83]. The structure of PP is the major factor behind the increase in both the rate of bromination and dehydro-bromination in comparison with PE [136,138].

The comparison of C1s peaks of before and after bromine gassing is shown in Figure 43. The shaded regions correspond to the broadened C1s peak due to bromine gassing represents the formation of bromine and oxygen functionalities.

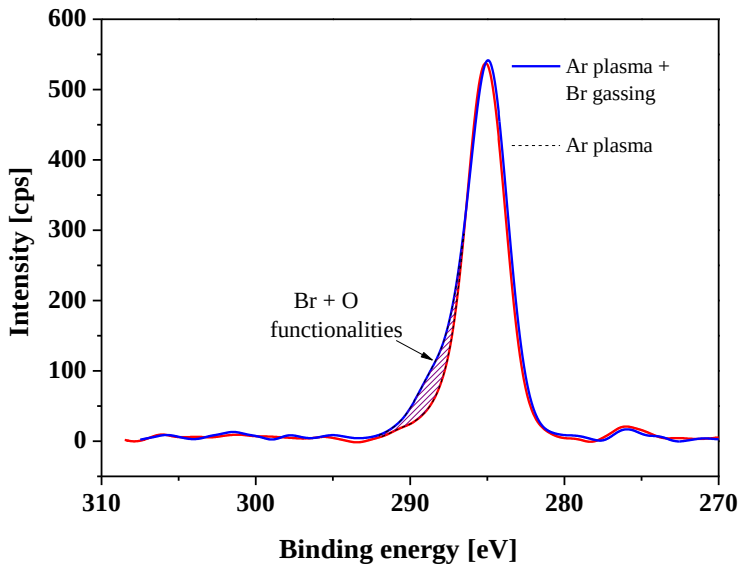

Figure 43: C1s peaks of PE- argon plasma treated (dotted lines) and PE-argon plasma treated for 5 min followed by bromine gassing for 15 min at 400 Pa (blue). The shaded regions represent the Br+O functionalities in LDPE.

The deconvolution of C1s peaks with C-Br bonds is very complex because of the fact that the binding energies of C-Br (286.3 eV) or C-Br_2 (288.5 eV) fall in the same range that of oxygen functionalities, C-O (286.6 eV), >C=O/CHO (ca. 288 eV) and O-C=O (289.2 eV). The existence of bromine peaks (Figure 41) therefore confirms the Br attachment to radical sites / olefinic double bonds on the polyolefin surface. The virgin foil was also treated with bromine gas for 15 min at 400 Pa inside the plasma chamber. The condensation of vapour can be ruled out because of the absence of any bromine peaks for untreated PE.

The introduction of covalently bonded bromine moieties onto the polyolefin surface could be understood as described above. It was expected that the reactions of Br_2 and O_2 preferably with C-radicals take place. Substitution of activated H (allyl position) or at tertiary C-atoms (polypropylene) by Br is also generally possible to some degree but these features are not present in PE. Presence of conjugated double bonds formed by radiation-induced dehydrogenation give also reasons for binding bromine as –CHBr–CHBr– moieties. The existence of double bonds could be identified after argon plasma treatment by UV-Vis spectroscopy (Figure 44).

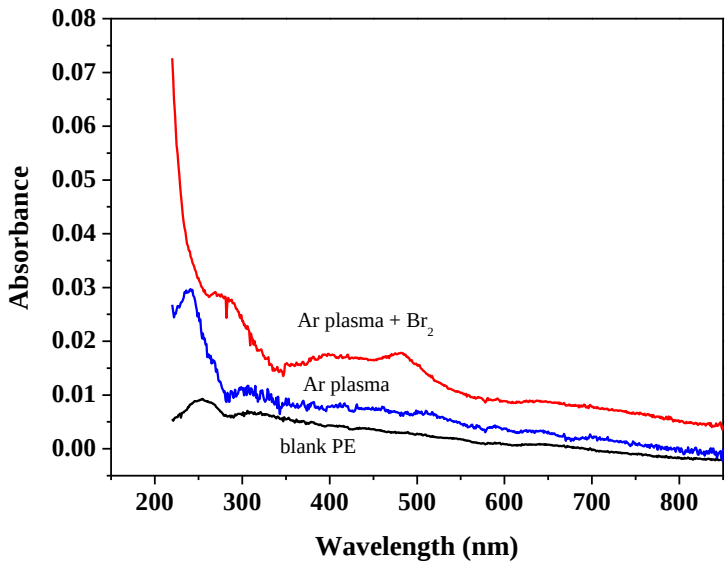

Figure 44: UV-Vis spectra of untreated (black), argon plasma exposed (blue) and then argon plasma treated followed by bromine gas (red) on LDPE.

The absorption was situated in the wavelength region of λ=200-250 nm characteristic for dienes and trienes. The C-Br absorption in the UV-C region is at λ=204 nm [134]. Wilken et al. had proposed a method to calculate the number of double bonds after bromination using XPS results [78,126]. Taking into account that one C=C bond can form 2 C-Br bonds, the total C=C bond concentration can be calculated from the bromine elemental composition found by XPS data. Assuming the polymer density of PE to be 0.92 g cm^{-3}, the number of C atoms for PE is 0.0575 mol/cm^3. The total C=C bonds in PE can be deduced from 0.5 • $[Br]_{at\%}$ • 0.0575 mol/cm^3. After 5 min argon plasma treatment and immediately followed by Br

gas for 15 min, the total C=C bond concentration by XPS data is $4.16 \cdot 10^{-3}$ mol/cm^3 for PE as shown in Table V in Appendix.

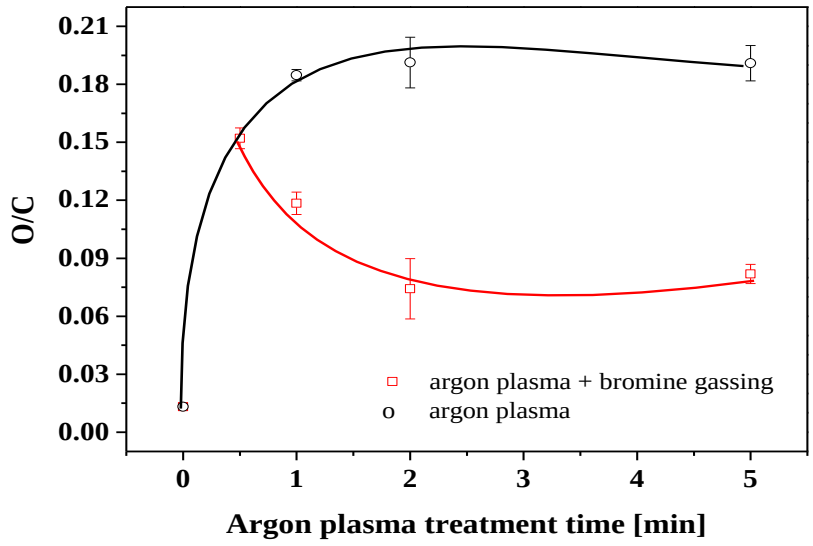

Figure 45: Comparison of O/C ratios for argon treated LDPE film (black) and LDPE treated with argon plasma and 15 min bromine gassing at 400 Pa (red).

In Figure 45 it can be seen that maximal 15-20% of oxygen is present at the surface of polyolefins as measured by XPS. However, in IR spectra O-indicating features are also absent within the whole sampling depth. Thus, also these oxygen containing groups are only situated at surface and in near-surface layers. The decrease of O/C for bromine gassed PE gives a clue that it may slow down/ hinder the auto-oxidation cycle in the first few nanometres of the sample. The decrease in O/C could be possible because of the radical quenching by bromine. The FTIR results also imply that the effect of bromine gassing is limited only to the surface layers.

It is assumed that bromine molecules cannot easily diffuse into the polymer under low-pressure conditions ($4 \cdot 10^2$ Pa) as also shown by the experiments with blank films. The diffusion is enhanced only using more amorphous polyethylene and high temperature [136]. Oxygen has more time for diffusion into the polyolefin bulk and the oxygen partial pressure at atmosphere is about $0.2 \cdot 10^5$ Pa. It was found by XPS that about 15% of O/C and 12% Br/C were measured after 30 s Ar plasma treatment followed by Br gassing, therefore, in sum

27% of hetero elements. Moreover, 30 s of Ar plasma treatment and after storage in ambient air for 1 day had produced 15% of O/C. Thus, it can be assumed that bromination under vacuum conditions of 30 s Ar plasma treated PE for 15 min and by storing it in ambient air for 1440 min (1 day) does not influence the oxygen introduction. Whereas, after time >1 min of argon plasma treatment followed by 15 min of bromine gassing decreases the oxygen introduction.

4.3. UV in-situ weathering of LDPE and simultaneous ESR measurement

It is understood that polymer starts to oxidize rapidly after the concentration of stabilizer drops under a certain value which is known as the critical stabilizer concentration. A polymer that contains the stabilizer only till critical concentration shows the same results as unstabilized sample. It can be expected that the critical concentration depends on the chemical structure of the stabilizer as well as on the stabilized polymer, and also on the degradation criterion tested for in the stabilized polymer sample. Moreover, the critical concentration could also depend on testing conditions used (temperature, irradiation intensity, etc.) [139,140]. From this point of view, ESR in-situ studies can be helpful in determining the optimal concentrations of stabilizers in relatively shorter weathering periods compared to natural weathering and simulated weathering tests in lab scale. UV in-situ weathering with simultaneous ESR could be a viable tool to study the early stages of weathering and ESR is a sensitive technique to analyse the radical formation. Radicals generated in polymers are the reason behind different physical and chemical property changes on the surface as well as bulk material. The free radicals act as intermediate between macromolecular chain scission and recombination reactions. Electron spin resonance (ESR) measurements can provide valuable information about structural and chemical properties of the more or less stable radicals. ESR signals represent the generation and recombination of dangling bonds, or free radicals in polymers because of their associated unpaired electrons. From the signal intensity, information on the type of radicals and on their concentrations can be found [141,142].

In this section, a simple method has been used to detect the presence of Hostavin N30 a hindered amine light stabilizer (HALS) enabled LDPE by ESR. It also focuses on the radical profiling of unstabilized and HALS stabilized LDPE is irradiated by UV and simultaneously measured by ESR. The basic mechanism of hostavin N30, an oligomeric HALS can be understood by Denisov cycle [143,144]. Figure 46 shows the plot of ESR signal intensity against the square root of the microwave power which is usually termed as power saturation curve. To reliably quantify ESR signals in samples with different relaxation times, spectra should be recorded in the region where signal intensity increases linearly with the square root of power [142].

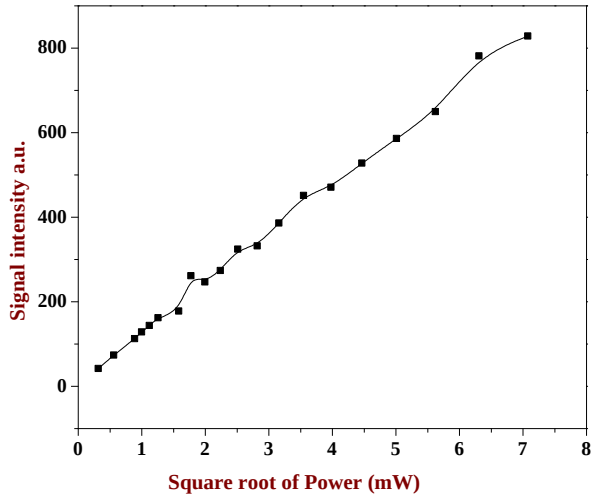

Figure 46: ESR signal intensity vs. Square root of power in mW

A sample of 1 wt% of HALS in LDPE is loaded into the sample holder and placed inside the field of electromagnet to see how the radical intensity changes with the power variation. A linear trend in the graph (Figure 46) denotes that there is no saturation of the spin system occurred within the available power in the spectrometer which indicates a shorter relaxation time of spin system. On the other hand, this also means that the HALS radicals have quite a long life time and is quite efficient.

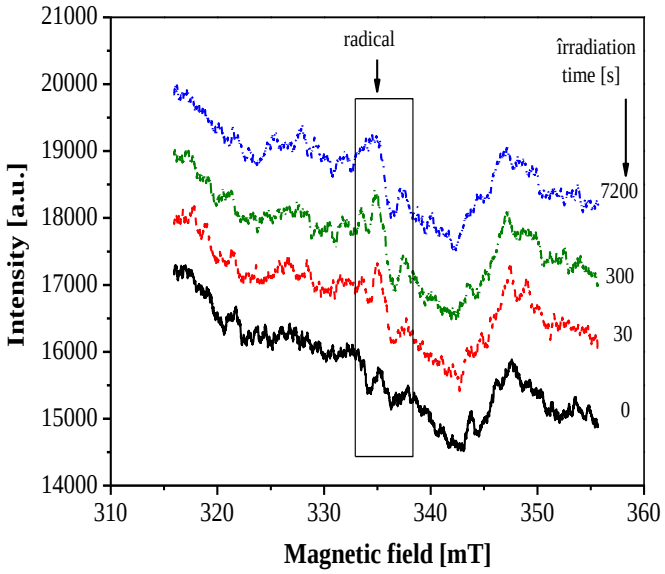

Figure 47: ESR signal in a.u. vs. magnetic field (mT) for neat LDPE irradiated at different times in sec

Figure 47 shows the ESR signal of unstabilized LDPE irradiated at different time periods. UV irradiation of unstabilized LDPE leads to Norrish reactions which have been discussed in Chapter 2.2. Several researches have been done so far on ESR investigations on UV irradiated polyethylene [141,145,146]. In general, two types of radicals are formed under Norrish I mechanism and if Norrish type II is followed then two molecules which can absorb UV light are formed. Both the pathways lead to the degradation of polyethylene.

An efficient stabilizer should be highly soluble in polymer, while its permeation inside the material should be slow. When the HALS stabilized LDPE irradiated by UV, it was found by ESR that the ageing is remarkably slowed down. In the work on HALS mechanisms, Gugumus documented that the performance of HALS in PP increased linearly with HALS concentration, while in LDPE the performance of HALS increased with the square root of the concentration [8].

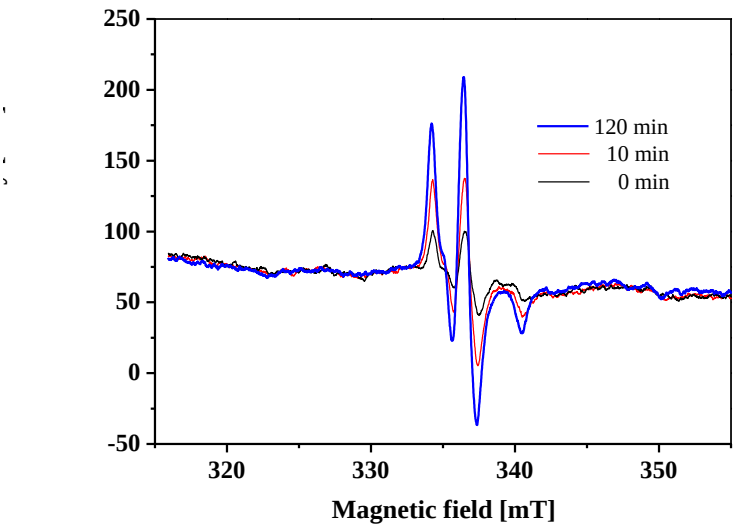

Figure 48: ESR spectra for UV irradiated 0.2 wt% Hostavin N 30 LDPE

Figure 48 shows the ESR signal of HALS stabilized LDPE and the appearance of such peak is due to the formation of nitroxyl free radicals from the polymer. The free radicals must result from the scission of N-CH_2 bonds by UV radiation followed by oxidation. Figure 49 shows the ESR radical intensity against the irradiation time in minute. It was found that 0.2, 0.8 and 1.0 wt% HALS LDPE can be ranked based on their signal intensities. These ESR signals reach saturation after 30 min and levels off till 120 min. So, the detection and ranking of concentration of HALS in LDPE can be achieved with just 30 min UV irradiation. The saturation intensities for the three concentrations are plotted as in Figure 50.

In the case of different stabilizers, the same method can be applied and ranking of stabilizers could be achieved in shorter time in comparison to outdoor weathering or analysing with other techniques.

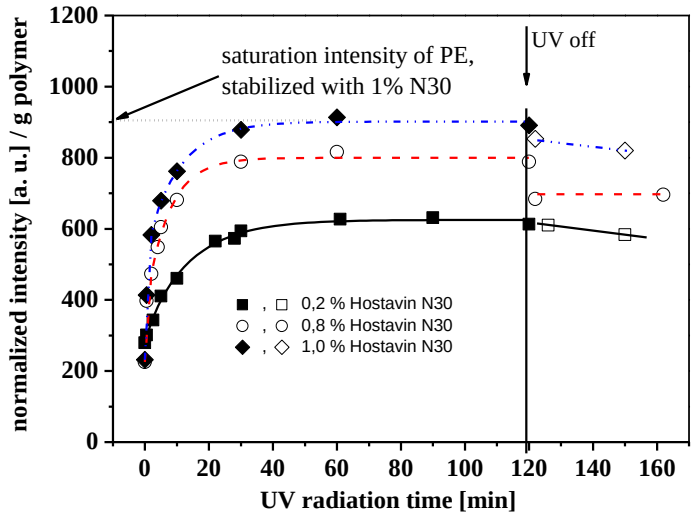

Figure 49: Radical intensity per gram for 0.2 (square), 0.8 (circle), and 1.0 (diamond) wt% Hostavin N 30 in LDPE against UV irradiation time

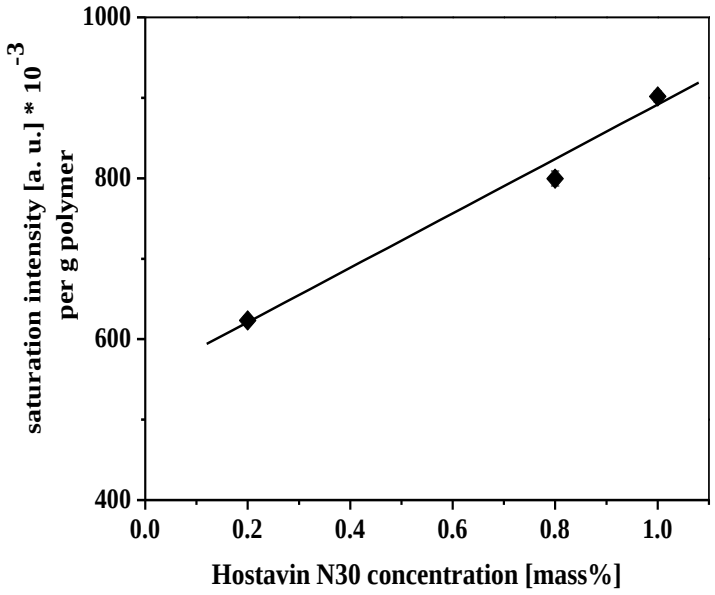

Figure 50: Saturated radical intensity per gram for 0.2, 0.8, and 1.0 wt% Hostavin N 30 in LDPE.

5. Conclusions

The main objective of this work is to understand how the photo-oxidation induced by artificial weathering, oxygen plasma treatment and UV in-situ weathering affects the lifetime of LDPE foils. The highlights of the study are, artificial weathering was carried out till the LDPE foils reached the state of mechanical disintegration. Secondly, oxygen plasma weathering was tried on LDPE to check for correlation with the effects of artificial weathering. Plasma surface modification of LDPE with bromine gas was tried to study the nature of surface photo-oxidation. Significant results were obtained.

5.1. Artificial weathering of LDPE

Firstly the LDPE foils are weathered in artificial weathering device at two different humid conditions: <15% RH and >90% RH. The surface effects of the weathered polymer were analysed by XPS and FTR in ATR mode. When analysed by XPS which measures the surface layers ca. 6 nm, it was found that with increase in weathering time the intensity of C-O, C=O and O-C=O bonds containing functional groups also increases. The effect of humidity is seen as more oxygen functional groups on the surface in comparison with the dry conditions. These findings are complemented with the results of ATR-FTIR. The analysis of carbonyl index gave an indication of photo-oxidation with increasing amounts of carbonyl groups such as aldehydes, ketones, carboxylic acids etc., within the 2.5 µm of the surface layers. For the samples weathered at <15% RH, foils could last till 32 days of exposure. Whereas, for the foils under high humidity >90% RH, foils could withstand only 12 days. Embrittlement was the reason behind these failures.

To understand the change in bulk properties, DRS and DSC was employed to see how embrittlement could shorten the lifetime of LDPE. It was found by DRS that due to the formation of radicals and subsequent photo-oxidation it was noticed that the weathering gives rise to dielectric active α_c and β relaxation processes which have a weak intensity for the non-polar unweathered LDPE. The generation of polar groups such as carbonyl is more

prominent in the amorphous region of the polymer. It was deduced that the dielectric loss increases with increasing weathering period and is associated with shifting of relaxation maxima towards higher temperature, which is interpreted as an indication of photo-oxidation. The prolonged weathering of LDPE under <15% RH leads to the total loss of its structural integrity by breaking into pieces due to embrittlement at the end of 32 days. Following interpretations were made:

1.) The dominant β relaxation process is due to the generation of polar groups in the amorphous regions,
2.) Dipolar motions in the crystallites during the earlier stages of weathering is less probable and is more prominent in the later stages due to chain scission and/or crosslinking, and
3.) Increase of crystallinity is observed which may be attributed to the ordered arrangement of shorter chains which is observed as crystalline α_c process.

The increasing degree of crystallization is in agreement with the DSC result. The dependence of activation energies and dielectric strengths of the α_c and β relaxation processes on the weathering time is also discussed in detail.

In the case of higher humidity, the foils could not be weathered beyond 12 days. The analysis of XPS and FTIR show that the presence of OH groups is increased with weathering time which could be an indication of humidity. When analyzed by DRS the effect of water is confirmed by the increased dielectric losses in comparison with dry conditions. The nature of hydrogen bonds with the polymer main chain and/ or the plasticization effect on the LDPE is still not clear. It was also presumed that the decrease of free volume in the amorphous regions due to the water permeation could also cause the immobility of short molecular chains which is also seen as the change in β relaxation processes, activation energies and dielectric strengths. The DSC measurements were not that conclusive as DRS which are attributed to the sensitiveness of the technique. It is concluded that dielectric relaxation spectroscopy could be a viable tool to analyse the effects of artificial weathering.

5.2. Oxygen plasma weathering and surface modification by Br gas

Plasma weathering is also termed as "ultra-accelerated ageing process". Since artificial weathering consumes time in weeks to give results, oxygen plasma was tried to check for correlation with the obtained weathering results. The maximum plasma treatment time is set as 4 h. The idea of correlating the results of artificial weathering and plasma weathering turned futile. However, the XPS results show some correlation. For example, when measured on the same day after weathering, 14% of oxygen functional groups were found after 25 days of artificial weathering under dry conditions. Likewise, 14% of oxygen atoms were found to be on the LDPE surface after 30 min of oxygen plasma at 50 W. Similar correlations with ATR-FTIR and tensile strength measurements could not be achieved. FTIR showed no significant change in carbonyl index and since oxygen plasma treatment affects only the top most surface layers (ca. 10 nm). The micro tensile studies indicate the foils were ductile with a change in the necking region for 0h and 4h treated samples and elongations at break were inconclusive.

Another attempt was also made to check if the polymer surface is modified what happens to the surface oxidation of the LDPE. Firstly, the LDPE was treated with argon plasma and then bromine vapor was passed without breaking the vacuum. It was found by XPS that bromine gas hinders or slows-down the photo-oxidation at the surface level. It was understood that the radicals and /or olefinic double bonds can react with bromine under low-pressure conditions. After 1 min of argon plasma treatment followed by 15 min of bromine gassing, the oxygen introduction decreased by 7%. Therefore, it can be assumed that the bromination does not reach the same sampling depths as oxygen and it reacts with radicals and/or double bonds which hinders /slows down the auto-oxidation process. This method can also be helpful in calculating the total C=C bonds in polyolefins. After 5 min argon plasma treatment and followed by Br gas for 15 min, the total C=C bond concentration by XPS data is $4.16 \cdot 10^{-3}$ mol/cm^3 for PE. The main disadvantage of this technique is the toxicity of bromine.

5.3. UV in-situ weathering of LDPE

When unstabilized LDPE were irradiated by UV and in-situ studies by ESR show that the radicals were formed based on Norrish type reactions and it was found that the radicals decrease with increasing exposure. In the case of 0.2, 0.8 and 1 wt% Hostavin N30 stabilized LDPE is irradiated, it was found that the nitroxyl radicals in stabilized LDPE absorb more UV radiation and hence the radical intensity increases with exposure time. It was found that Hostavin N30 is highly resistant to UV radiation in air.

5.4. Recommendations for future research

Till this date, varieties of polymers with different thicknesses are being studied making artificial weathering tests more challenging. When polymer composites are taken into consideration, understanding of weathering become a daunting task. This work has produced some results which have potential to develop into some models for simulation work with following assumption: A semi-crystalline polymer of 40 µm thicknesses with 50% crystallinity under ambient humid conditions may withstand 32 days. The maximum oxygen diffusion can be set as 14% and UV radiant exposure can be kept as a variable parameter. This may help in finding a formula for polymer service lifetime.

The oxygen plasma experiments can be tried with different power values and at high vacuum conditions. DRS of oxygen plasma treated polymers could be possible when it is tried with thin films.

The UV in-situ weathering by ESR can be tried in ranking of concentrations in stabilized polymers and ranking of stabilizers in a considerable shorter irradiation time is also viable.

II Appendix

Table I: The values of C-C/C-H, C-O, C=O and O-C=O functional groups for LDPE weathered under <15% RH.

Weathering days	C–C/C-H	C–O	C=O	O–C=O
0	92.2	5.0	2.0	0.6
7	87.2	8.1	2.2	1.9
14	85.7	8.0	3.2	1.6
32	80.8	9.3	3.3	3.2

Table II: The values of C-C/C-H, C-O, C=O and O-C=O functional groups for LDPE weathered under >90% RH.

Weathering days	C–C	C–O	C=O	O–C=O
0	92.2	5.0	2.0	0.6
2	87.0	8.9	1.9	1.7
7	81.9	11.3	2.7	2.8
14	77.4	12.5	4.1	4.5
29	77.1	12.3	3.9	4.7

Table III: The values of C-C, C-O, C=O, and O-C=O functional groups in % for LDPE treated by oxygen plasma at 50 W.

O_2 plasma time (min)	C–C	C–O	C=O	O–C=O
0	92.2	5.0	2.0	0.6
30	82.8	9.6	4.3	3.2
60	80.4	10.5	5.0	3.9
120	79.3	10.7	5.3	4.7
240	79.3	10.4	6.0	4.2

Table IV. Values of bromine elemental composition for PE films after argon plasma treatment and immediately followed by bromine gassing.

Argon plasma treatment time (min)	Br/C	C=C bonds concentration ($*10^{-3}$ mol/cm³)
0	0	0
0.5	0.1	3.6
1	0.12	4.1
2	0.12	4.2
5	0.1	4.1

Table V. Comparison of oxygen atoms for argon plasma treated PE foil before and after bromine gassing.

Argon plasma treatment time (min)	Argon plasma	Argon plasma followed by bromine gassing	
	O [%]	O [%]	Br [%]
0	1.3	1.3	0
1	18.5	11.8	11
2	19.1	7.4	13
5	19.1	8.2	12

6. Publications from the work

1. Maalolan Ramanujam*, Volker Wachtendorf, Purv Purohit, Renate Mix, Andreas Schönhals, Jörg Friedrich, *A detailed dielectric relaxation study of artificial UV weathered low density polyethylene*, **Thermochimica Acta, Vol. 530, pp. 73-78, 2012**.

2. Maalolan Ramanujam, Renate Mix, Manfred Wagner, Jörg Friedrich*, *Effect of bromine gassing after argon plasma treatment of polyolefins*, **Journal of adhesion science and technology**, (**accepted**).

3. Maalolan Ramanujam*, Volker Wachtendorf, Purv Purohit, Renate Mix, Andreas Schönhals, Jörg Friedrich, *A detailed dielectric relaxation study of artificial UV weathered low density polyethylene with >90% humidity*, (to be submitted).

4. Maalolan Ramanujam*, Volker Wachtendorf, Renate Mix, Andreas Schönhals, Jörg Friedrich, *Influence of UV weathering and humidity on surface and bulk properties of LDPE*, in **Natural and artificial ageing of polymers**, 5th European Weathering Symposium, Ed. Thomas Reichert, **ISBN 978-3-9813136-2-8**.

5**.** Renate Mix, Maalolan Ramanujam, Volker Wachtendorf, Jörg Friedrich*, *New ways for investigation for polymer weathering by ESR*, in **Natural and artificial ageing of polymers**, 5th European Weathering Symposium, Ed. Thomas Reichert, **ISBN 978-3-9813136-2-8**.

Poster presentations:

1. Maalolan Ramanujam, Volker Wachtendorf, Renate Mix, Andreas Schönhals, Jörg Friedrich, *Effect of UV radiation and moisture on artificially weathered PMMA and LDPE*, ASPM 2010, Loeben, Austria, Sep 8-10, 2010.

2. Maalolan Ramanujam, Renate Mix, Jörg Friedrich, *Argon plasma treatment of PP and PE – Trapping of radicals using NO gas*, Plasma Surface Engineering 2010, Garmisch-Partenkirchen, Germany, Sep 13-17, 2010.

III. References

[1] CMAI, 2010.

[2] P. A. Dilara and D. Briassoulis, J. Agric. Engg. Res. 76, 309-321, 2000.

[3] H. F. Mark, Encyclopedia of Polymer Science and Technology, 3 ed. John Wiley & sons, 2004.

[4] J. F. Rabek. Polymer Photodegradation: Mechanisms and Experimental Methods, Chapman and Hall, 1995.

[5] J. L Bolland, Trans. Faraday Soc., 44, 669,1948.

[6] J. L. Bolland, Quart. Rev., 3,1,1949.

[7] L. Bateman, Quart. Rev., 8,147,1954.

[8] F. Gugumus, Angew. Makromol. Chem., 182,111,1990.

[9] J. Sampers, J. Polym. Degrad. Stabil. 76, pp. 455-465, 2002.

[10] G. Wypych, Handbook of Material Weathering, 2 ed. ChemTec publishing, 1990.

[11] L. K. Massey, The Effects of UV light and Weathering on Plastics and Elastomers, 2 ed., William Andrew publishing, 2007.

[12] S. A. Jabarin and E. A. Lofgren, J. Appl. Polym. Sci. 53(4), 411-423, 1994.

[13] A. Davis and D. Sims, Weathering of polymers. Ultraviolet radiation. Applied science publishers, London, 1983.

[14] J. Attwood et al., Polym. Degrad. Stabil. 91, 3407-15, 2006.

[15] R. Geetha et al., Polym. Degrad. Stabil, 19, 279-292, 1987.

[16] H. Hamid, M. B. Amin, A. G. Maadhah, Handbook of polymer degradation. Marcel-Dekker, New York, 1992.

[17] M. Sebaa, C. Servens and J. Pouyet, J. Appl. Polym. Sci., 47(11), 1897-1903, 1993.

[18] A. Torikai, A. Takeuchi, S. Nagaya. K. Fueki. J. Polym. Photochem. 7,199,1986.

[19] A. Tidjani, Polym. Degrad. Stabil. 68(3), 465-469, 2000.

[20] A. Tidjani, R. Arnaud and A. Dasilva, J. Appl. Polym. Sci, 47(2), 211-216, 1993.

[21] C. David, M. Trojan and A. Daro, Polym. Degrad. Stabil. 37(3), 233-245, 1992.

[22] J. V. Gulmine, P.R. Janissek, H. M. Heise and L. Akcelrud, Polym. Degrad. Stabil. 79(1), 385-397, 2003.

[23] Gugumus, F., Developments in the UV-stabilisation of polymers. In *Developments in Polymer Stabilisation—1*, ed. G. Scott. Applied Science Publishers, London, 1979.

[24] Castejón, M.L., Tiemblo P., Gómez-Elvira J.M., Polym. Degrad. Stab., 71, 99, 2001.

[25] A. C. Tavares et al. Polym. Degrad. Stabil. 81, 367-73, 2002.

[26] B. Y. Zhao et al. J. Appl. Polym. Sci., 88(1), 12-16, 2003.

[27] J. E. Pikett. Polym Prepints, 42(1), 344, 2001.

[28] ATLAS Weathering Testing Guidebook.

[29] J. W. Summers and E. B. Robinovitch, J. Vinyl Technol. 5(3), 1983.

[30] A. A. Basfar and K. M. Idriss Ali. Polym. Degrad. Stabil. 91, 437- 443, 2006.

[31] A. L. Andrady, J. E. Pegram, J. Appl. Polym. Sci. 39, 363–370, 1990.

[32] L. C. Mendes et al. Polym. Degrad. Stabil., 79, 371, 2001.

[33] P. Pagés et al. J. Appl. Polym. Sci., 60,153, 1996.

[34] S. Suzuki et al. The 23rd Japan Congress on Materials Research: Non -metallic Materials, Tokyo, p. 293, 1989.

[35] Weiss Umwelttechnik GmbH , http://www.wut.com

[36] CIE publication no. 85, 1989.

[37] A. A. Basfar et al. / Polym. Degrad. Stabil. 82, 229–234, 2003.

[38] G. Yanai, A. Ram, and J. Miltz, J. Appl. Polym. Sci., 57, 303–310, 1995.

[39] S. Nakatsuka and A. Andrady, J. Environ. Polym. Degrad. 2, 161–167, 1994.

[40] M. Salvalaggio et al. Polym. Degrad. Stabil. 91, 2775-85, 2006.

[41] D. Briggs, Surface Analysis of Polymers by XPS and Static SIMS, Cambridge University Press, 1998.

[42] T. Corrales et al. J. Photochem. Photobiol A: Chem., 147, 213–224, 2002.

[43] N. M. Stark, L. M. Matuana, Polym. Degrade. Stabil. 86, 1–9, 2004.

[44] F. Gugumus, Polym. Degrad.Stabil. 76, 329– 340, 2002.

[45] M. M. El-Awady, J. Appl.Polym.Sci., 87, 2365–2371, 2003.

[46] P. Pagès et al. J. Appl.Polym.Sci., 60, 153–159, 1996.

[47] S. Massey, A. Adnot and D. Roy, J. Appl. Polym. Sci., 92, 3830-38, 2004.

[48] S. Massey et al., E. Polym. Lett. 1(8), 506-11, 2007.

[49] D. Milicevic, S. Trifunovic, M. Popovic, T. V. Milic, E. Suljovrujic. Nucl. Instrum. Meth. B 260, 603-612, 2007.

[50] E. Suljovrujic, G. Stamboliev, D. Kostoski. Radiat. Phys. Chem. 66,149-154, 2003.

[51] V. Djokovic, D. Kostoski, S. Galovic, M. D. Dramicanin, Z. K. Popovic. J. Polym. Degrad. Stabil. 61, 73-77,1998.

[52] E. Suljovrujic. Polymer 43, 5969-78, 2002.

[53] E. Suljovrujic, Z. K. Popovic, D. Kostoski, J. Dojcilovic. J. Polym. Degrad. Stabil. 71 367-73, 2001.

[54] F. P. La Mantia. Radiat. Phys. Chem. 23, 699-702, 1984.

[55] F. P. La Mantia, R. Schifani. J. Polym. Degrad. Stabil. 10, 67-78,1985.

[56] F. Kremer, A. Schönhals, (eds.), Broadband Dielectric Spectroscopy, Springer Verlag, 2002.

[57] O. van den Berg, W. G. F. Sengers, W. F. Jager, S. J. Picken, M. Wübbenhorst, Macromolecules 37, 2460, 2004.

[58] A. Torikai, A. Takeuchi, S. Nagaya. K. Fueki. J. Polym. Photochem. 7,199, 1996.

[59] N. G. McCrum, B. E. Read, G. Williams. An Elastic and Dielectric Effects in Polymeric Solids; Wiley: New York, 1967 (Reprinted by Dover 1991).

[60] A. Schönhals, H. Goering, F. R. Costa, U. Wagenknecht, G. Heinrich. Macromolecules 42, 4165-4174, 2009.

[61] P. Frübing, D. Blischke, R. G. Multhaupt, M. S. Khalil. J. Phys. D: Appl. Phys. 34, 3051-3057, 2001.

[62] N. C. Billingham, P. Prentice and T. J. Walker, J. Polym. Sci. Symp. 57, 287-97, 1976.

[63] M. Mansfield, R. Boyd, J. Polym. Sci. Polym. Phys. 16,1227–1252, 1978.

[64] K.S. Rohr, H.W. Spieß, Macromolecules 24,5288, 1991.

[65] W.G. Hu, C. Boeffel, K.S. Rohr, Macromolecules 32, 1611–1619, 1999.

[66] R.H. Boyd, G. Smith, Polymer Dynamics and Relaxation, Cambridge University Press, 2007.

[67] E.L. Leguenza, P.C.N. Scarpal, D.K. Das-Gupta, IEEE Trans. Dielectr. Electr. Insul. 9, 507, 2002.

[68] J. Friedrich, J. Gähde, A. Nather, Plaste u. Kautsch. 28, 420-425, 1981.

[69] J. Friedrich and H. Frommelt, Acta Chim. Hung. 125, 165-175, 1988.

[70] J. Friedrich et al. Intern. J. Mater. Sci. Vol. 13,43-56, 1990.

[71] J. Friedrich et al. P*olym. Degrad. Stabil.* 31, 97, 1991.

[72] N. Shahidzadeh-Ahmadi, F. Arefi-Khonsari and J. Amouroux , J. Mater. Chem. 5, 229-236, 1995.

[73] J. R. White and A. Turnbull, J. Mat. Sci. 29, 584-613, 1994.

[74] J. Friedrich, Plasma chemistry of Polymer Surfaces: Advanced Techniques for Surface Design, Wiley VCH , 2012.

[75] B.B. Cooray and G. Scott, in "Developments in Polymer Stabilisation-2", edited by G. Scott (Applied Science) p. 53, London, 1980.

[76] F. Poncin-Epaillard, B. Chevet and J. C. Brosse, J. Adhes. Sci. Technol. 8, 455-468 1994.

[77] F. Poncin-Epaillard, B. Chevet, and J. C. Brosse, J. Appl. Polym Sci. 52, 1047-1061 1994.

[78] R. Wilken, A. Holländer and J. Behnisch, Macromol. 31, 7613-7617, 1998.

[79] A. Holländer, S. Kröpke and F. Pippig, Surf. Interface Anal. 40, 379-385, 2008.

[80] R. Wilken, A. Holländer and J. Behnisch, Surf. Coat. Technol. 116-119, 991-995, 1999.

[81] J. F. Friedrich, *Plasma modification of polymers*, in: Polymer-Solid Interfaces, J. J. Pireaux, P. Bertrand, J. L. Bredas (Eds.), Institute of Physics Publishing, Bristol, pp. 443-454,1992.

[82] J. F. Elman, L. J. Gerenser, K. E. Goppert-Berarducci and J. M. Pochan, Macromolecules 23, 3922-3928, 1999.

[83] S. Balamurugan, A. B. Mandale, S. Badrinarayanan and S. P. Vernekar, Polymer 42, 2501-2512, 2001.

[84] N. Chanunpanich, A. Ulman, Y. M. Strzhemechny, S. A. Schwarz, A. Janke, H. G. Braun and T. Kratzmüller, Langmuir 15, 2089-2094, 1999.

[85] J. F. Friedrich, S. Wettmarshausen and M. Hennecke, Surf. Coat. Technol. 203, 3647-3655, 2009.

[86] F. Niyazi and I. V. Savenkova, *New Concepts in Polymer Science-Photodegradation and Light Stabilization of Heterochain Polymers*. G. E. Zaikov (Ed.), VSP, 2006.

[87] N. S. Allen et al., J. Polym. Degrad. Stabil. 61, 183-199, 1998.

[88] www.specialchem4adhesives.com

[89] J. L. Hodgson and M. L. Coote. Macromolecules, 43: 4573-4583, 2010.

[90] P. Gijsman, J. Hennekens and D. Tummers, Polym. Degrade.Stabil. 39, 225, 1993.

[91] O. Haillant and J. Lemaire, Polym. Degrade. Stabil. 91, 2748-2760, 2006.

[92] Allen, N.S., Polym. Degrad. Stabil. 2 (2), 129–135, 1980.

[93] Allen, N.S. Degradation and Stabilization of Polyolefines. Applied Science Publishers, London and New York, 1983.

[94] A. A. Basfar, K. M. Idriss Ali, S. M. Mofti, Polym. Degrad. Stabil. 82 (2), 229–234, 2003.

[95] P. Gijsman and A. Dozeman, Polym. Degrade. Stabil, 53, 45-50, 1996.

[96] M. Scoponi, S. Cimmino and M. Kaci, Polymer, 41, 7969-80, 2000.

[97] J. Pilar et al. Polym. Degrade. Stabil. 96, 847-862, 2011.

[98] Determination of optical parameters with relevance to bacterial sterilization, MSc. Thesis (Self) submitted to University of Stuttgart, 2008.

[99] R.H. Boyd, Polymer 26, 323–347, 1985.

[100] R.H. Boyd, Macromolecules 17, 903–911, 1984.

[101] C.R. Ashcraft, R.H. Boyd, J. Polym. Sci. Polym. Phys. 14, 2153–2193, 1976.

[102] A. Torikai et al. J. Polym. Photochem. 7, 199, 1986.

[103] R.S. Stein, J. Macromol. Sci. Phys. B, 8, 29–40, 1973.

[104] Y. Sato, T. Yashiro, J. Appl. Polym. Sci. 22, 2141–2153, 1978.

[105] R.G. Mathews, A.P. Unwin, I.M. Ward, G. Capaccio, J. Macromol. Sci. Phys. B 38, 123–143, 1999.

[106] S. Havriliak, S. Negami. Polymer, 8, 161, 1967.

[107] Havriliak, S. Negami. Polymer, 10, 859, 1969.

[108] S. Havriliak, S. Negami, J. Polym. Sci. C-Polym.Symp., 99, 1966.

[109] H. Vogel. Physikalische Zeitschrift, 22, 645, 1921.

[110] G. S. Fulcher. J. Amer. Cer. Soc. 8, 339, 1925.

[111] G. Tammann, W. Hesse. Zeitschrift für Anorganische und Allgemeine Chemie, 156, 245, 1926.

[112] W.K. Fisher, J.C. Corelli, J. Polym. Sci. Polym. Phys. 19, 2465–2493, 1981.

[113] B. Fayolle, X. Colin, L. Audouin, J. Verdu, Polym. Degrad. Stab. 92, 232–238, 2007.

[114] A. Danch, W. Osoba, F. Stelzer, Eur. Polym. J. 39, pp. 2051-58, 2001.

[115] S. Lightfoot, G. Xu, Polymer plastics technology and Engineering, 32:1-2, pp. 21-31, 2006.

[116] K. Pathmanathan, G. P. Johari, R. K. Chan, Polymer 27, 1907, 1986.

[117] B. Wunderlich, J. Chem. Phys. 37, 2429, 1962.

[118] N. Sprang, D. Theirich and J. Engermann, Surf. Coat. Technol. 74, 689, 1995.

[119] H. J. Busscher et al. J. Colloids. Surf. 9, 319, 1984.

[120] I. Banik et al, Polymer, 44, 1163, 2003.

[121] M. Morra et al. Ed. Plasma surface modification: relevance to adhesion. Utrecht: VSP; 1994.

[122] M. Kuzuya, J. Niwa and H. Ito, Macromolecules, 26, 1990, 1993.

[123] I. Retzko et al. J. Electron. Spectroscop. Relat. Phenom. 121, 111, 2000.

[124] A. N. Bhoj, M. J. Kushner, IEEE Trans. Plasma Sci. 33(2): 250–1, 2005.

[125] S. M. Desai and R. P. Singh, Adv. Polym. Sci. 169, 231-293, 2004.

[126] R. Wilken, A. Holländer and J. Behnisch, Plasmas and Polymers 7, 185-205, 2002.

[127] L. J. Gerenser, J. Adhes. Sci. Tech. 1, 303-318, 1987.

[128] B. K. Kim, K. S. Kim, C. E. Park and C. M. Ryu, J. Adhesion Sci. Technol. 16, 509-521, 2002.

[129] J. F. Friedrich, G. Kühn and J. Gähde, Acta Polymerica 30, 470-477, 1979.

[130] R. M. France and R. D. Short, J. Chem. Soc., Faraday Trans. 93, 3173-3178, 1997.

[131] R. H. Hansen and H. Schonhorn, J. Polym. Sci. B4, 203-211, 1966.

[132] M. Hudis, J. Appl. Polym. Sci. 16, 2397-2411, 1972.

[133] B. K. Kim et al. J. Adhesion Sci. Technol. 16, 509-521, 2002.

[134] D. J. Carlson, R. Brousseau, C. Zhang and D. M. Wiles, Polym. Degrad. Stabil. 17, 303-318, 1987.

[135] D. J. Carlson and J. Lacoste, Polym. Degrad. Stabil. 32, 377-386, 1991.

[136] M. A. McRae and W. F. Maddams, Die Makromolekulare Chemie 177, 461-471 1976.

[137] V. M. Möhring, K. Seevogel and G. Fink, Fresenius Z. Anal. Chem. 323, 330-333 1986.

[138] E. Fanghänel (Ed.), *Organikum*, Wiley-VCH, 22nd Ed., Weinheim, 2004.

[139] V. Mika, L. Preisler, J. Sodomka, Polym. Degrad. Stabil. 28, 215-225, 1990.

[140] P. Jiang-Qing, C. Song, Polym. Degrad. Stabil. 40, 375-8, 1993.

[141] K. Tsuji, T. Seiki, J. Polym. Sci., Polym. Lett. 7, 839, 1969.

[142] B. Randy, J. F. Rabek, *ESR Spectroscopy in Polymer Research*, Springer, Berlin 1977.

[143] E. T. Denisov, Dev. Polym. Degrad. 5, 23, 1982.

[144] J. L. Hodgson and M. L. Coote, Macromolecules, 43, 4573-4583, 2010.

[145] S. Ohnishi, S. Sugimoto, I. Nitta, J. Chem. Phys. 39, 2647, 1963.

[146] B. Ranby, H. Yoshida, J. Polymer Sci. Part C 12, 263, 1966.

List of Figures

Figure 18: O-C=O groups in (%) for LDPE weathered at <15% RH (black) and >90% RH (red) against weathering days.

Figure 19: Dielectric loss ε'' vs. temperature at a frequency of 1000 Hz for 0 (square), 3 (pentagon), 6 (hexagon), 12 (circle), 25 (star) and 32 (triangle) days of weathering at <15% RH. The three relaxation processes namely α_c, β, γ appears in order of decreasing temperature (The γ relaxation is observed only for 25 (star) and 32 days (triangle) weathered LDPE) in the given temperature range.

Figure 20: Dielectric loss ε'' vs. temperature at a frequency of 1000 Hz for 0 (black), 3 (red), 6 (blue) and 12 (cyan) days weathered LDPE at >90% RH.

Figure 21: Comparison of dielectric losses at 1000 Hz for dry and humid weathered LDPE.

Figure 22: Dielectric loss vs. temperature after 25 days of weathering for different frequencies: 10 Hz (star), 100 Hz (diamond), 1000 Hz (triangle), 10000 Hz (Inverted triangle) and 100000 Hz (square).

Figure 23: f_{max} for the three relaxation processes: α_c (diamond), β (triangle) and γ (circle) for 25 days weathered LDPE at 1000 Hz. The solid line is a linear fit to the corresponding data for each relaxation process.

Figure 24: Relaxation rates f_{max} vs 1/T for the β relaxation process for different weathering times, 3 days (square), 6 days (circle), 12 days (triangle), 25 days (hexagon), and 32 days (star). The solid lines are fits of the Arrhenius equation to the corresponding data. The inset shows E_a as a function of the weathering time for the β relaxation.

Figure 25: Relaxation rates f_{max} vs. 1/T for the β relaxation process for different weathering times, 3 days (black), 6 days (red) and 12 days (blue) weathered at >90% RH. The solid lines are fits of the Arrhenius equation to the corresponding data. The inset shows the activation energy (E_a) as a function of the weathering time for the β relaxation.

Figure 26: Relaxation rates f_{max} vs. 1/T for α_c relaxation processes for 3 days (square), 6 days (circle), 12 days (triangle), 25 days (pentagon) and 32 days (diamond). The solid lines are linear fits of the Arrhenius equation and slope gives the activation energy. The inset shows the activation energy (E_a) as a function of weathering time for α_c relaxation.

Figure 27: Relaxation rates f_{max} vs. 1/T for α_c relaxation processes for 3 days (black), 6 days (red), 12 days (blue) weathered at >90% RH. The solid lines are linear fits of the Arrhenius equation and slope gives the activation energy. The inset shows the activation energy (E_a) as a function of weathering time for α_c relaxation.

Figure 28: ε' (circles) and ε'' (squares) vs. temperature for three days weathered LDPE at f = 1 kHz indicating the dielectric strengths of β and α_c relaxation. The absolute values of ε´are subjected to errors because no gold electrodes are deposited at the samples.

Figure 29: Dielectric strengths of the α_c relaxation vs. weathering period. The inset gives $\Delta\varepsilon_\beta$ vs. the weathering time.

Figure 30: The dielectric strengths for α and β relaxation modes for LDPE weathered at 60°C with >90% RH

Curriculum Vitae

Personal details

Name	:	Maalolan Ramanujam
Date of Birth	:	09-05-1982
Nationality	:	Indian
Place of Birth	:	Tiruchirapalli, Tamilnadu
Marital Status	:	Married
Languages	:	English (fluent), Tamil (native), German (Mittelstufe), Hindi (basic)

Educational qualification

Mar 2009 – Feb 2012	:	PhD student in BAM – Federal Institute for Materials Research and Testing, Berlin, Germany
Oct 2005 – Jan 2008	:	M. Sc. (Physics), University of Stuttgart, Stuttgart, Germany
Jun 1999 – Jun 2002	:	B. Sc. (Physics), National College, affiliated to Bharathidasan University, Tiruchirapalli, India
May 1998 – May 1999	:	Higher secondary XII standard, Vailankanni Raj Matric. Hr. Sec. School, Tiruchirapalli, India
May 1995 – May 1996	:	Matriculation X standard, Vailankanni Raj Matric. Hr. Sec. School, Tiruchirapalli, India

Work experience

Mar 2012 – till date	:	Plasma process development – Physicist, Nagarjuna Spawnt GmbH, Wolfen-Bitterfeld, Germany
Feb 2008 – Feb 2009	:	Research assistant, Fraunhofer Institute-IGB, Stuttgart, Germany
April 2003 – July 2005	:	Copy Editor, Alden Pre-press services India, Ltd. India